Bismuth vanadate-based semiconductor photocatalysts a short critical review on the efficiency and the mechanism of photodegradation of organic pollutants

Olivier Monfort, Gustav Plesch

Bismuth vanadate-based semiconductor photocatalysts: a short critical review on the efficiency and the mechanism of photodegradation of organic pollutants

Olivier Monfort[a,b,*], Gustav Plesch[b]

[a]Univ Rennes, Ecole Nationale Supérieure de Chimie de Rennes, CNRS, ISCR (Institut des Sciences Chimiques de Rennes) – UMR 6226, F-35000 Rennes, France

[b]Comenius University in Bratislava, Faculty of Natural Sciences, Department of Inorganic Chemistry, Ilkovicova 6, Mlynska Dolina, 842 15 Bratislava IV, Slovakia

[*]correspondence: (email) olivier.monfort@ensc-rennes.fr, (tel.) +33223238134
(address) ENSCR, 11 allée de Beaulieu, CS 50 837, 35708 Rennes Cedex 7, France

Abstract

The number of publications on photocatalytic bismuth vanadate-based materials is constantly increasing. Indeed, bismuth vanadate is gaining stronger interest in the photochemical community since it is a solar-driven photocatalyst. However, the efficiency of $BiVO_4$-based photocatalyst under sunlight is questionable: in most of the studies investigating the photodegradation of organic pollutants, only few works identify the by-products and evaluate the real efficiency of $BiVO_4$-based materials. This short review aims to (i) present briefly the principles of photocatalysis and define the photocatalytic efficiency, (ii) discuss the formation of reactive species involved in the photocatalytic degradation process of pollutants and thus the corresponding photodegradation mechanism could be determined. All these points are developed in a comprehensive discussion by focusing especially on pure, doped and composite $BiVO_4$. Therefore, this review exhibits a critical overview on different $BiVO_4$-based photocatalytic systems with their real efficiency. This is a necessary knowledge for potential implementation of $BiVO_4$ materials in environmental applications at larger scale than laboratory conditions.

Keywords: $BiVO_4$; photocatalysis; efficiency; mechanism; organic pollutant

Acknowledgement

The authors wish to acknowledge the financial support provided by the Scientific Grant Agency of the Slovak Republic through the project VEGA 1/0276/15.

1 Introduction to semiconductor photocatalysis

1.1 Generalities and principles

Since the last industrial revolution, our natural environment has been considerably damaged and is still being deteriorated due to the human activity, in particularly factories in the field of textile, chemistry, agriculture and pharmacy (Azenha et al. 2013; Gaya 2014; Hinojosa-Reyes et al. 2015). For example, the quality of water (underground and at the surface) is alarming because the production of dyes, pesticides, fertilizers, drugs and synthetic chemicals from these industries releases organic pollutants such as aromatic compounds, azo and sulfur derivatives and active pharmaceutical ingredients (Azenha et al. 2013; Gaya 2014; Hinojosa-Reyes et al. 2015; Larsson 2014). These contaminants could be toxic not only for human beings but also for plants and animals, and this concern has pushed environmental agencies and national governments to legislate and impose stringent measures in order to limit the diffusion of pollutants in our environment (Gaya 2014). However, limiting the pollution does not remediate the damages already caused to the planet. Therefore, for the abatement of pollutants in water, photocatalysis has been found to be a viable solution and a good alternative to traditional biological, chemical and physical decontamination technologies (Azenha et al. 2013; Gaya 2014).

The photocatalysis can be classified into two categories: homogeneous and heterogeneous photocatalysis. In this review, we focus on heterogeneous photocatalysis using solid inorganic materials. Heterogeneous photocatalysis is an eco-friendly process where semiconductors are considered, so far, as the most promising photocatalysts (Azenha et al. 2013; Gaya 2014). A photocatalyst is a material that can induce reaction upon direct light absorption or photosensitisation (Gaya 2014). Under an irradiation of energy hv equal or larger than the energy band-gap E_g (separating the conduction band CB and the valence band

VB) of the semiconductor, electrons (e^-) migrate to the CB leaving holes (h^+) in the VB, thus the material is photoactivated due to the formation of e^-/h^+ pairs. The photogenerated e^- and h^+ are the basis of the heterogeneous photocatalysis using semiconductors (SC) (Azenha et al. 2013; Gaya 2014; Hermann 1999; Ibhadon and Fitzpatrick 2013; Linsebigler et al. 1995).

However, after photon absorption by the SC, the formation of photogenerated e^-/h^+ pair is in competition with charge recombination leading to the release of absorbed energy in the form of heat or light (Azenha et al. 2013; Gaya 2014; Hermann 1999; Ibhadon and Fitzpatrick 2013; Linsebigler et al. 1995). The fate of electrons and holes can follow several pathways that affect the photocatalytic efficiency. For a photocatalytic reaction, it is mandatory that the photogenerated charges reach the surface of the photocatalyst where they react with adsorbed species behaving either as electron donor (D) or acceptor (A) (Azenha et al. 2013; Gaya 2014; Hermann 1999; Ibhadon and Fitzpatrick 2013; Linsebigler et al. 1995). It is worth to notice that, at the photocatalyst surface, h^+ and e^- exist in the form of defects or are trapped. The resulted redox reactions give rise to intermediates or final products (A^- and D^+) as seen in **Fig. 1**. The feasibility of a photocatalytic reaction depends on the position of the CB and VB edges of the photocatalyst and the redox potential energy of the adsorbed reactants (Gaya 2014; Hermann 1999; Ibhadon and Fitzpatrick 2013; Linsebigler et al. 1995; Litter 1999). Indeed the potential of adsorbed donor should be lower (more negative) than the energy of the valence band maximum (VBM), and similarly, the potential of adsorbed acceptor should be higher (more positive) than the energy of the conduction band minimum (CBM) as illustrated in **Fig. 1** (Gaya 2014; Hermann 1999; Ibhadon and Fitzpatrick 2013; Linsebigler et al. 1995; Litter 1999).

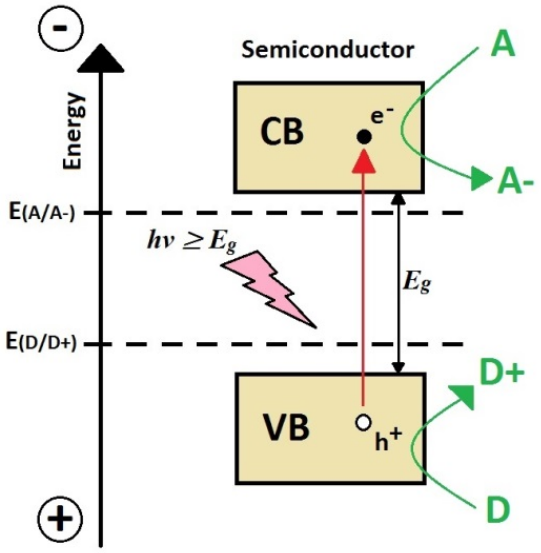

Fig. 1 Band structure of a semiconductor and its photoactivation under irradiation of energy *hv* where A and D are adsorbed reactants having different redox potentials

Usually, the degradation of organic pollutants catalysed by a semiconductor is an oxidative process using either directly the oxidising power of photogenerated holes or indirectly through oxidation by reactive oxygen species (ROS). These ROS are formed by reaction of oxygen and/or water with photogenerated e^-/h^+ pair (Azenha et al. 2013, Koltsakidou et al. 2017). The photooxidation through h^+ is not kinetically favored in the presence of ROS since these strong oxidising species react much faster. Therefore, for efficient pollutant degradation, i.e. its full mineralisation, the formation of ROS radicals (**eqs. 1–8**) is crucial (Azenha et al. 2013; Edge 2013; Gaya 2014; Hinojosa-Reyes et al. 2015; Lazar et al. 2012; Lelario et al. 2016). The use of ROS radicals for the photooxidative degradation of organic pollutants is so-called advanced oxidation process (AOP). The most powerful ROS are hydroxyl radicals ($OH^\bullet$) that can be formed from photogenerated h^+ and surface hydroxyl (on photocatalyst) or even water (hydroxide anions). Hydroxyl radicals have a strong redox potential *vs.* Normal Hydrogen Electrode (NHE) and they react non-selectively and rapidly

with most organic substrates (Azenha et al. 2013; Edge 2013; Gaya 2014; Hinojosa-Reyes et al. 2015; Lazar et al. 2012; Polczynski et al. 2013; Teoh et al. 2012; Wood 1988).

$$SC + h\nu \rightarrow e^- + h^+ \quad (1)$$

$$OH^-_{ads} + h^+ \rightarrow OH^\bullet \quad E(OH^-_{ads}/OH^\bullet) = 2.8 \text{ V } vs. \text{ NHE} \quad (2)$$

$$H_2O + h^+ \rightarrow OH^\bullet + H^+ \quad E(OH^-_{water}/OH^\bullet) > 2.8 \text{ V } vs. \text{ NHE} \quad (3)$$

Other radical species can be formed by reaction between photogenerated charges, already formed radicals and other chemical species present in the photocatalytic system as, for instance, in the following equations:

$$O_2 + e^- \rightarrow O_2^{\bullet-} \quad E(O_2/O_2^{\bullet-}) = -0.33 \text{ V } vs. \text{ NHE} \quad (4)$$

$$O_2^{\bullet-} + H^+ \rightarrow HO_2^\bullet \quad (5)$$

$$2\ OH^\bullet \rightarrow H_2O_2 \quad (6)$$

$$H_2O_2 + e^- \rightarrow HO^\bullet + OH^- \quad (7)$$

$$H_2O + O_2^{\bullet-} \rightarrow HO_2^\bullet + OH^- \quad (8)$$

Semiconductor photocatalysts can be used not only for the degradation/mineralisation of organic pollutants but also in other various processes such as water splitting for the production of O_2 and H_2 (**Fig. 2**), partial oxidation, reductive dehalogenation, etc. (Teoh et al. 2012).

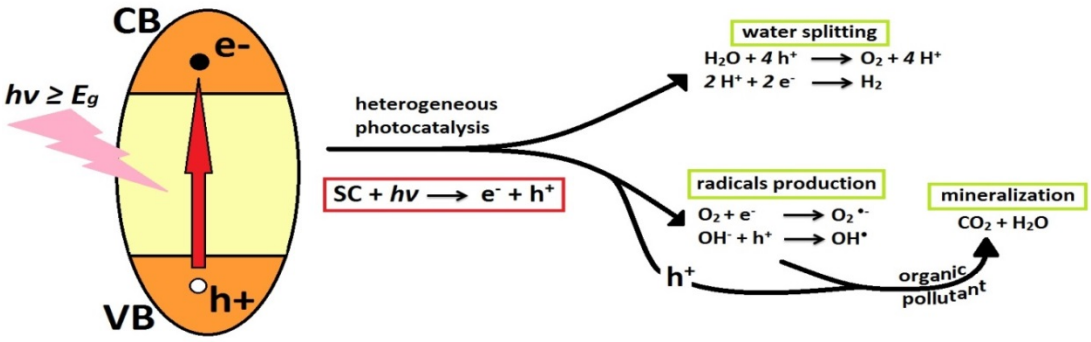

Fig. 2 Photocatalytic processes occuring in semiconductor material

1.2 Semiconductor photocatalysts and performance issue

By far, among the semiconductor materials including metal oxides (TiO_2, WO_3, ZnO, α-Fe_2O_3, $SrTiO_3$, …) and sulfides (ZnS, CdS, …), titania-based photocatalysts are the most used due to their low cost, non-toxicity, chemical stability, ease of synthesis and relative high photocatalytic efficiency compared to other inorganic semiconductors that are toxic, photocorrosive or less efficient like CdS, ZnO and α-Fe_2O_3, respectively (Gaya 2014). However, pure TiO_2 is photoactive only under ultra-violet (UV) radiations, which represent only about 5% of the natural solar light (Hashimoto et al. 2005; Hermann 1999; Lazar et al. 2012; Ni et al. 2007). As a consequence, scientists have focused their research either on the improvement of TiO_2 photocatalyst by shifting its photoactivity toward the visible region (which represents about 50% of the sunlight) or on the elaboration of new photocatalysts that are activated under visible light (Hashimoto et al. 2005; Ni et al. 2007). For the latter case, bismuth vanadate ($BiVO_4$) is a serious candidate (presented in **section 3**) and this material is discussed throughout this short review. Since the last decade, the number of works devoted to $BiVO_4$ has considerably increased and even some reviews are partly devoted to this promising semiconductor photocatalysts, especially in the field of water oxidation (Bhat and Jang 2017;

Gholipour et al. 2015; Huang et al. 2014a; Li et al. 2013; Lianos 2017; Liao et al. 2012; Moniz et al. 2015; Park et al. 2013). However, the real efficiency of photooxidative degradation of organic pollutants using $BiVO_4$ is questionable: in most of the works on $BiVO_4$ photocatalysis, only the concentration in initial pollutant is followed and not that of by-products that are formed and that could be more toxic than the original targeted pollutant (discussed in **section 4**). Therefore, for the comparison of $BiVO_4$ photocatalyst with the most popular and commercially available TiO_2, the results should be taken with caution since the superiority of bismuth vanadate (and more generally any promising semiconductor photocatalyst) over titania is often based on tests using a single organic substrate or on a narrow selection of test reactions which are not representative for adequate comparison: indeed many factors cannot be validated in a single test assay (Ibhadon and Fitzpatrick 2013; Teoh et al. 2012). Thus, this short review is devoted to a critical discussion of the real efficiency of visible light-driven $BiVO_4$-based photocatalysts based mainly on the photodegradation mechanism involved in such photooxidative processes – reflecting the ability of full mineralisation of organic pollutants.

2 Notions of photocatalytic efficiency and mechanism

2.1 Photocatalytic efficiency

The photocatalytic efficiency can be expressed in two different ways that are intimately linked. The first one is the quantum yield Φ that measures the efficiency of a photocatalytic process and which is defined as the number of events occurring per photon absorbed by the system (Serpone and Salinaro1999):

$$\phi = \frac{Amount\ (mol) of\ reactant\ consumed\ or\ product\ formed\ in\ the\ system}{Amount\ (einstein) of\ photons\ absorbed\ by\ the\ photocatalyst\ at\ wavelength\ \lambda} \quad (9)$$

It needs to be stressed that, as expressed in **eq. 9**, it is the absorbed photons and not the incident ones that initiate and drive a photocatalytic process. However, the ability to measure the actual absorbed photons is very difficult in heterogeneous systems due to scattering of light by the semiconductor surface. Therefore, it is usually assumed that all the light is absorbed and the efficiency is quoted as apparent quantum yield. In addition, e^-/h^+ recombination and back-donation process – after charge transfer from the adsorbed species to the semiconductor surface – limit the overall quantum yield of photocatalytic reactions (Gaya 2014; Hermann 1999; Ibhadon and Fitzpatrick 2013; Linsebigler et al. 1995; Litter 1999).

The second possibility to define the photocatalytic efficiency is to calculate the percentage of mineralisation. Indeed the mineralisation efficiency is a concrete way to evaluate the total abatment of organic pollutant, which is the focus of **section 4**. In addition, the determination of the photocatalytic efficiency in the removal of organic pollutants depends on the type of irradiation and semiconductor photocatalyst, the susceptibility of the pollutant to photooxidative degradation, and it is also related to the photocatalytic mechanism (Gaya 2014). Among the parameters just cited previously, the targeted pollutant is one of the most important. Indeed, its chemical structure as well as its electronic properties can influence the efficiency of a photooxidative degradation (Gaya 2014; Ibhadon and Fitzpatrick 2013; Teoh et al. 2012), sometimes requiring longer irradiation time (Lazar et al. 2012; Lopez-Alvarez et al. 2011). For instance, aliphatic compounds are more susceptible to photooxidation than aromatic substances since a single bond is easier to break than a double bond (Gaya 2014; Ibhadon and Fitzpatrick 2013; Teoh et al. 2012). In addition, the degree of substitution of a pollutant is also a crucial parameter in its ability to undergo photooxidation (Fang et al. 2013; Lowry and Johnson 2004; O'Carroll et al. 2013; Quiroga et al. 2009; Rybnikova et al. 2016). Indeed, in the case of polychlorinated biphenyls (PCBs), which are classified as persistent organic pollutant (resistance to natural degradation and thus

contaminating all natural compartments – especially soil, ground and surface water), photooxidation is difficult to achieve due to chlorine substituents hindering the aromatic ring, which cannot be attacked by ROS radicals (Fang et al. 2013; Lowry and Johnson 2004; O'Carroll et al. 2013; Quiroga et al. 2009; Rybnikova et al. 2016). However, many scientists have already successfully mineralised pollutants such as pesticides, BTX, pharmaceutical compounds that are a threat for human health (An et al. 2011; Lopez-Alvarez et al. 2011; Zhang et al. 2006). Thus, the study of photocatalytic mechanism and mineralisation efficiency is an important issue to evolve from laboratory research to pilot scale experiments, i.e. from fundamental to applied science.

2.2 Photocatalytic mechanism

2.2.1 Identification of oxidative species

Apart from the nature of photocatalyst, irradiation and pollutant, the photocatalytic mechanism is probably the most crucial information since it governs the photocatalytic efficiency. Indeed the mechanism gives a real idea on the probability of mineralisation. By studying the mechanism, it is possible to identify the main oxidative species that are associated to an oxidising power. From this identification, it is possible to deduce the ability (or not) to degrade a target pollutant and its degradation products into CO_2 and H_2O. The oxidative species e.g. h^+ and ROS can be identified by several means directly and indirectly.

As direct determination method, electron paramagnetic resonance (EPR) is the most used technique since particular species such as DMPO (5,5-dimethyl-1-pyrroline-N-oxide) are used as spin trapping agents for ROS radicals (Chen et al. 2008; Hu et al. 2011; Hu et al. 2015; Kanigaridou et al. 2016; Lin et al. 2012; Mohapatra and Parida 2014; Saison et al. 2015; Sun et al. 2015; Zhang et al. 2015; Zhang et al. 2018). By using EPR method,

superoxide and hydroxyl radicals are especially identified in the photocatalytic system due to their characteristic 6-line and 4-line peaks, respectively (Chen et al. 2008; Hu et al. 2011; Hu et al. 2015; Kanigaridou et al. 2016; Lin et al. 2012; Mohapatra and Parida 2014; Saison et al. 2015; Sun et al. 2015; Zhang et al. 2015; Zhang et al. 2018). Another technique which can be considered as direct method for the identification of $OH^{\bullet}$ radicals is the photoluminescence technique involving terephtalic acid (TA) or coumarin (Hu et al. 2015; Lamdab et al. 2016; Lin et al. 2012; Lu et al. 2014; Mohapatra and Parida 2014). By introducing TA in the presence of hydroxyl radicals, a fluorescent compound (2-hydroxyterephtalate) is formed and a signal at 426nm appears by prior excitation at 315nm. The fluorescence intensity in the photoluminescent spectrum increases with irradiation time.

Indirect methods are usually chosen for the identification of oxidative species during a photocatalytic reaction. Indeed such methods are easy to implement as, for example, the charge scavenging technique. Chemical substances that scavenge particular oxidative species are deliberately introduced in the photocatalytic system and the overall influence on the degradation rate is followed (Chen et al. 2008; Hu et al. 2017; Huang et al. 2017; Katsumata et al. 2013; Li et al. 2015; Lin et al. 2012; Liu et al. 2017; Liu et al. 2018; Xue et al. 2017; Zhai et al. 2017; Zhang et al. 2018). By this mean, hydroxyl radicals can be identified using iso-propanol or tert-butanol; superoxide radicals can be highlighted by using p-benzoquinone while photogenerated hole can be directly scavenged by ammonium oxalate or EDTA (ethylene-diamine-tetra-acetate). Another technique to identify oxidative species involved in photocatalytic mechanism is to make assumptions based on theoretical calculation of photocatalyst band structure, but such a method is not viable (Guo et al. 2016; Lamdab et al. 2016).

2.2.2 Identification of by-products

In order to state the photocatalytic efficiency and to confirm the ability of full mineralisation, the final state of the photocatalytic system should be analysed to search for degradation products (if any). For this, a commonly used method is the total organic carbon (TOC) analysis from which the amount of totally oxidised carbon (CO_2) at a time *t* in the photocatalytic system is calculated (Hu et al. 2007; Koltsakidou et al. 2017; Lin et al. 2012; Lopes et al. 2016; Luo et al. 2016; Mohapatra and Parida 2014; Lu et al. 2014). Such analysis does not give information on the identity of the different organic molecules present in the system at time *t*. Therefore, the remaining degradation products should be identified using other methods such as gas and liquid chromatography (GC and LC), mass spectrometry (MS), nuclear magnetic resonance (NMR), and other analytical methods (Hu et al. 2011; Kanigaridou et al. 2016; Koltsakidou et al. 2017; Lelario et al. 2016; Liu et al. 2018; Lopes et al. 2016; Lu et al. 2014; Sun et al. 2015; Zhang et al. 2015; Zhang et al. 2018). Chromatographic techniques (LC and GC) are based on the difference in retention times of the products. The retention time is characteristic for each chemical compound for given stationary and eluent phases under given conditions. In addition, MS can identify chemical products and by-products based on their mass-to-charge ratio (*m/z*). Indeed, mass spectrometry implies to ionise molecules in order to identify the mass of their different ion fragments with accuracy depending on the technique used e.g. high resolution MS or MS/MS tandem. However, these analytical techniques can be coupled in order to improve the identification of degradation products that are eventually present in the treated system, especially if TOC analysis confirms presence of organic matter.

All these analytical methods cited just before can be also used to study the kinetic of photocatalytic processes. However, the study of kinetics is more complex since during the photocatalytic process, many additional parameters should be taken into account such as the

formation of secondary radical species and the competition between initial and formed species (Hu et al. 2007; Teoh et al. 2012). With respect to this degree of complexity, the kinetics of photooxidative degradation processes are still the matter of discussion. Usually, many scientists claim that photocatalytic processes obey the Langmuir-Hinshelwood model, which is a model based on the adsorption of reactants onto the photocatalyst surface, while other researchers reclaim for proper experimental evidences to validate this model (Kumar et al. 2008; Lazar et al. 2012).

3 Brief background of bismuth vanadate ($BiVO_4$)

Bismuth vanadate fulfills several requirements that are necessary for an ideal photocatalyst (Gan et al. 2014; Ibhadon and Fitzpatrick 2013; Tolod et al. 2017). Among them, non-toxicity, resistance to chemical corrosion and visible light harvesting are the most important. The latter parameter is crucial for potential applications in renewable technologies since the energy coming from the Sun could be used to trigger green photocatalytic processes. Although further studies seem necessary to evaluate the benefits of $BiVO_4$, bismuth vanadate and its derivative materials are considered as good candidates for environmental applications.

3.1 Structure of bismuth vanadate

Concerning its structural characteristics, $BiVO_4$ exists in three polymorphs: monoclinic scheelite-like, tetragonal scheelite-like and tetragonal zircon-like structures with E_g of 2.40, 2.34 and 2.90 eV, respectively (Gan et al. 2014; Li et al. 2013a; Park et al. 2013; Tolod et al. 2017; Xu et al. 2011). The crystal structures are composed of $[VO_4]$ tetrahedra and $[BiO_8]$ polyhedra where V(V) and Bi(III) are in the centre of the units. In the scheelite

phases, each *[BiO_8]* is surrounded by eight *[VO_4]* whereas in zircon structure, Bi units are surrounded by only six *[VO_4]* (Park et al. 2013). The difference between monoclinic and tetragonal scheelite structures is based on the local environment of Bi and V that is more distorted in the monoclinic structure (Park et al. 2013). In addition the tetragonal structure is a high temperature phase exhibiting reversible transition to monoclinic scheelite at 255 °C (Park et al. 2013; Tolod et al. 2017). Moreover, irreversible transition between tetragonal zircon and tetragonal scheelite happens at about 400-500 °C (Park et al. 2013; Tolod et al. 2017). Of the two $BiVO_4$ polymorphs stable at room temperature, monoclinic scheelite-like structure exhibits the best photoactivity due to better photon absorption. This improved light absorption results from smaller E_g and more distorted V and Bi units promoting charge carrier transport compared to tetragonal-zircon structure (Park et al. 2013; Tolod et al. 2017; Tokunaga et al. 2001; Xu et al. 2011). Bismuth vanadate has a direct band gap where the upward of VB and the lowering of CB is the result of hybridization of O 2p with Bi 6s orbitals and predominant contribution of V 3d orbitals, respectively (Chen et al. 2010; Gan et al. 2014; Li et al. 2013a; Park et al. 2013; Tolod et al. 2017).

3.2 Photophysical properties

The photocatalytic activity of $BiVO_4$ depends strongly on its crystalline phase but also on the exposed crystal facets (Gan et al. 2014). Indeed the different crystal facets of $BiVO_4$ influence the thermodynamic and kinetic factors of a photoreaction by modifying important properties such as the preferential adsorption of a reactant, the migration of charge carriers and the desorption of products (Gan et al. 2014; Teoh et al. 2012). For monoclinic $BiVO_4$, the *{010}* and *{110}* crystal facets provide reduction and oxidation sites, respectively, thus these facets have redox functions in which photogenerated electrons and holes are available (Li et

al. 2013; Tachikawa et al. 2016; Tan et al. 2016; Tan et al. 2017; Thalluri et al. 2014; Xi and Ye 2010). However, Tan et al. (2016, 2017) observed that the photooxidation properties of monoclinic bismuth vanadate are better for *{010}* dominant-$BiVO_4$ (facet with reduction sites). They explained this fact by fast electron transfer to acceptor species favored by more e^- available at larger *{010}* surface, therefore e^-/h^+ is promoted and photogenerated h^+ at *{110}* surface reacts more efficiently with donor species (Tan et al. 2016; Tan et al. 2017). For better understanding, **Fig. 3** shows the different charge transfer in both *{010}* and *{110}* dominant $BiVO_4$.

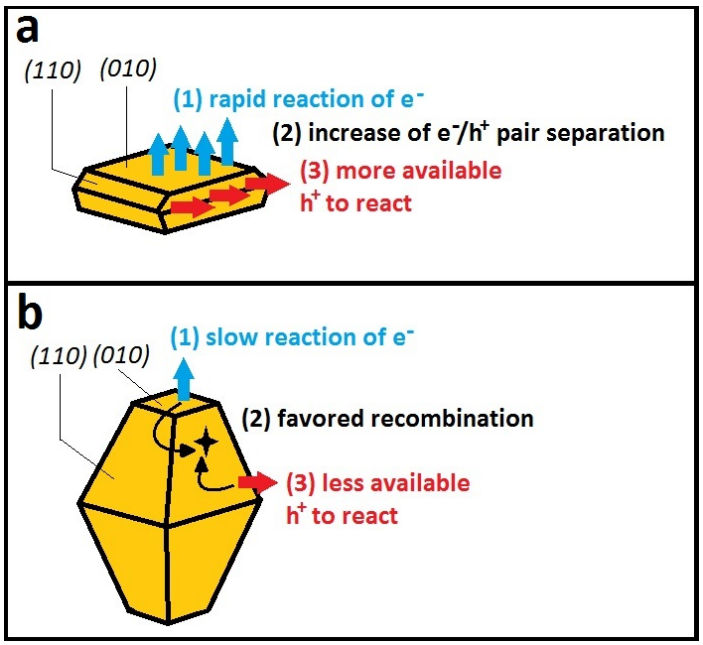

Fig. 3 Charge transfer mechanism in $BiVO_4$ with (a) *{010}*-dominated facet and (b) *{110}*-dominated facet

Despites the advantages of $BiVO_4$ presented above, several drawbacks are responsible of low efficiency of $BiVO_4$ photocatalyst (Gan et al. 2014; Tolod et al. 2017). First, bismuth vanadate suffers of poor electron mobility and high e^-/h^+ recombination (Gan et al. 2014; Tolod et al. 2017). These main disadvantages are due to the $BiVO_4$ structure where *[VO_4]* tetrahedra are not connected to each other, and also to the strong localisation of V 3d orbitals

that constitute the CB (Tolod et al. 2017). In addition, $BiVO_4$ has a short hole diffusion length (70−100 nm) that compromises the optimisation of light harvesting according to the optical penetration depth principle (Tolod et al. 2017).

3.3 Synthesis of bismuth vanadate

The way of preparation of bismuth vanadate is crucial in the performance of $BiVO_4$ photocatalyst (Chiarello and Selli 2010; Gan et al. 2014). Indeed, many parameters such as phase formation, morphology, crystal facets, surface area and surface defects depend directly on the synthesis procedure. Thus, the synthesis influences significantly e^-/h^+ transport and interfacial kinetics (Chiarello and Selli 2010; Gan et al. 2014; Xu et al. 2011). Bismuth vanadate was first synthesised by solid state and melting reactions in 1963 (Chen et al. 2010; Roth and Waring 1963). To date, the most commonly used synthesis methods for the preparation of $BiVO_4$ in the form of film and powder are metal organic decomposition (MOD), precipitation and hydrothermal methods (Galembeck and Alves 2000; Hubert-Pfalzgraf 2003; Ke et al. 2008; Park et al. 2013; Sayama et al. 2003; Thurston et al. 2004; Xu et al. 2011). Other techniques can be also used such as electrochemical and sol-gel processes but they are less common (Hofmann et al. 2015; Pookmanee et al. 2012; Seabold and Choi 2012; Wang et al. 2016). Most of these preparation methods allow the use of dopants and/or surfactants into the reactive mixture in order to tune the chemical composition and to control the morphology of $BiVO_4$ materials (Park et al. 2013). A surfactant, also called structure directing agent, is often a polymer that affects the micro- and nano-structure of a material by adjusting its morphology, surface area, porosity, crystallinity, and crystal phase formation (Garcia-Perez et al. 2012; Xu et al. 2011). Examples of surfactant are poly-ethylene glycol

(PEG), Triton X-100, Pluronic P123 and F127, cetyl-trimethyl-ammonium bromide (CTAB) and poly-vinyl pyrrolidone (PVP).

4 $BiVO_4$-based photocatalysts

As a semiconductor photocatalyst, $BiVO_4$-based materials are mainly studied in the form of powder or film. Most of the published works on $BiVO_4$ photocatalyst are actually devoted to systems containing powder suspension. For environmental applications, immobilisation of photocatalyst on rigid supports such as glass, polymer or ceramic is crucial in order to avoid the post-separation difficulties associated with the slurry form (Azenha et al. 2013; Ibhadon and Fitzpatrick 2013, Lazar et al. 2012).

4.1 Pure $BiVO_4$

$BiVO_4$ is a relatively recent material in the field of photocatalysis, therefore most of the literature is devoted to optimisation of its physical characteristics (morphology, porosity, etc…) for potential photocatalytic applications. Consequently only basic photocatalytic tests are performed. To introduce the photooxidative properties of $BiVO_4$, many works discussed the photocatalytic efficiency by following initial concentration of model pollutants without taking care of detailed photodegradation pathways. However, to discuss the photocatalytic efficiency, a statement cannot be made based on rough observation (such as the monitoring of initial pollutant concentration) or even from assumptions on photocatalytic mechanism.

Table 1 summarises published articles devoted to photodegradation of organic pollutants using pure $BiVO_4$ (this list is not exhaustive). Only few groups have studied in details the mineralisation of pollutant photodegradation using pure $BiVO_4$ photocatalyst. For

instance Lopes et al. (2016) have studied by TOC and MS the photooxidative degradation of methylene blue under visible light. They have found out that pure $BiVO_4$ mineralised 65% of the dye while the degradation products are compounds containing hydroxylated aromatic or cleaved chromophore functions (Lopes et al. 2016). From one work to another, differences between photocatalytic efficiencies can appear, but they arise from many reasons such as the way of synthesis or the parameters of photocatalytic system (type of irradiation, kind of pollutant, concentrations in photocatalyst and pollutant, etc.). Deeper studies are therefore necessary to clear out all these uncertainties on $BiVO_4$ efficiency before considering its use in environmental applications.

Table 1. Summary of photocatalytic degradation of organic pollutants using pure $BiVO_4$.

$BiVO_4$ form	**Pollutant**	**Irradiation**	**Efficiency**	**Ref.**
Powder (2 g/L)	Rhodamine B (5 mg/L)	Solar	C/C_0(60min) = 0.1	Wang et al. (2016)
Powder (1g/L)	Methyl Orange ($4 \cdot 10^{-5}$ M)	Visible	C/C_0(100min) = 0	Hofmann et al. (2015)
Powder (1 g/L)	Rhodamine B (5 mg/L)	Solar	C/C_0(240min) = 0.3	Garcia-Perez et al. (2012)
Powder (1 g/L)	Methylene Blue (10mg/L)	Visible	C/C_0(150 min) = 0.30	Fan et al. (2012)
Powder (1 g/L)	Methylene Blue (20 mg/L)	Visible	C/C_0(120min) = 0.25	Fan et al. (2011)
Powder (2 g/L)	Ibuprofen (10 mg/L)	Solar	C/C_0(40min) = 0.1	Li et al. (2016a)
Powder (10 mM)	Methyl Orange (40 mg/L)	Visible	C/C_0(30min) = 0.1	Zhou et al. (2006)
Powder (2.5 g/L)	Rhodamine B (25 mg/L)	Solar	C/C_0(60min) = 0.2	Guo et al. (2010)
Powder (1 g/L)	Methylene Blue (10 mg/L)	Solar	C/C_0(120min) = 0.1	Lu et al. (2015)
Powder (0.5 g/L)	Methyl Orange (10^{-5} M)	Visible	C/C_0(120min) = 0.2	Jiang et al.

				(2012)
Powder (1 g/L)	Methylene Blue (10 ppm)	Visible	C/C_0(180min) = 0.15	Li et al. (2008)
Powder (0.5 g/L)	Rhodamine B (5 mg/L)	Visible	C/C_0(120min) = 0.1	Ran et al. (2015)
Powder (2 g/L)	Methylene Blue (10 mg/L)	Solar	C/C_0(180min) = 0.05	Shen et al. (2010)
Powder (1 g/L)	Methylene Blue (10 mg/L)	Solar	C/C_0(180min) = 0.05	Chen et al. (2016)
Powder (1 g/L)	Phenol (0.2 mM)	Visible	C/C_0(240min) = 0.1	Jiang et al. (2011)
Powder (1 g/L)	Methylene Blue (10 mg/L)	Solar	C/C_0(240min) = 0.1	Liu et al. (2015)
Film (1.5 cm^2)	Rhodamine B (10^{-5} M)	Solar	C/C_0(180min) = 0.5	Monfort et al. (2017a)
Powder (0.5 g/L)	Methylene Blue (5 mg/L)	Visible	C/C_0(180min) = 0.5	Lopes et al. (2015)

Concerning the mechanism of pollutant degradation, numerous works can be found, but authors often confuse efficiency and mechanism (refs. in **Table 1**). For example, they evaluate the efficiency in mineralisation by extrapolating the discussion on the mechanism and the formation of final by-products such as CO_2. Vice versa, mechanism is often determined based on the efficiency of mineralisation (the produced CO_2) suggesting a hypothetical mechanistic degradation pathway. To evaluate the mechanism in a safer way, the most popular technique is the use of charge scavengers. However, the results could be very different from one work to another, where some scientists have stated the main oxidation species as hydroxyl radicals while other researchers have found that superoxide radicals have the higher contribution in the degradation of the studied pollutant (refs. in **Table 1**). In addition, Monfort et al. (2017a) have identified, also by charge scavenger, the photogenerated holes as the main photooxidative species of pure $BiVO_4$. This observation is in adequation

with the work of Saison et al. (2015) whom has proven this fact by EPR results which is even a more reliable method. But why different mechanisms are identified for the same photocatalyst? This is a critical issue since many parameters can affect the observed photochemical properties. Under normal conditions (25 °C; *pH* = 0), $BiVO_4$ is not able to produce hydroxyl and superoxide radicals (**Fig. 4**). Indeed, the conduction band minimum (CBM) of $BiVO_4$ is too much positive (0 V *vs.* SHE) for allowing the formation of superoxide radicals (-0.33 V *vs.* NHE), i.e. $E°(O_2/O_2^{\bullet-})$ is not within E_g of $BiVO_4$. Moreover, due to overpotential losses, hydroxyl radicals cannot be formed since the valence band maximum (VBM) of bismuth vanadate is too close of $E°(OH^{\bullet}/H_2O)$ which is around 2.4 V *vs.* NHE.

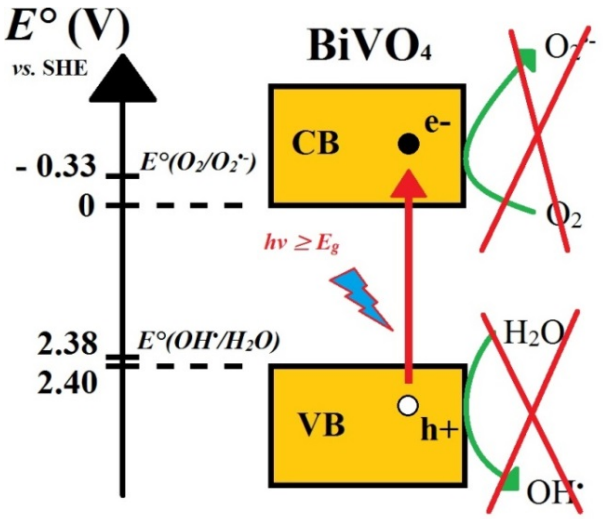

Fig. 4 Band structure of pure $BiVO_4$ associated with the energetic value of band edge positions and ROS radicals formation

However, the *pH* of photocatalytic medium can shift the energetic position of redox potentials for a given reaction while the presence of a dye in the photocatalytic system can sensitise the photocatalyst. In the latter case, the observed mechanism does not result from the intrinsic properties of the photocatalyst. Indeed, the excited electrons of the dye can be transferred to the CB of $BiVO_4$ and the injected electrons can subsequently produce $O_2^{\bullet-}$ (**Fig.**

5). Therefore superoxide radicals could become the main oxidative species in the photodegradation of organic dye. In order to solve this issue, the study of photodegradation and sensitisation mechanisms based on organic dye should be coupled to another pollutant in order to evaluate intrinsic properties of pure bismuth vanadate (Monfort et al. 2017b; Odling and Robertson 2016).

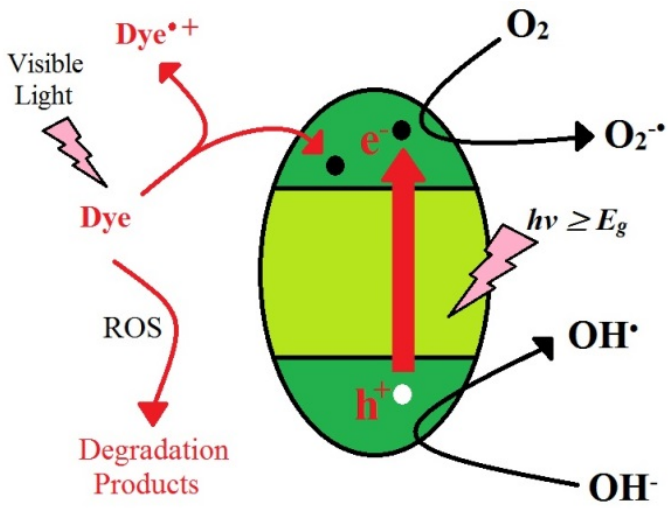

Fig. 5 Sensitization of a photocatalyst by a dye and its subsequent degradation

Despites the works attempting to discuss photocatalytic mechanism based on experimental observations in presence of $BiVO_4$, many other published works often base their discussion on assumptions, calculations, already published data or even speculations (Hofmann et al. 2015; Liu et al. 2015). But without further experimental data to complete these theoretical results, a reliable mechanism cannot be determined.

4.2 Doped $BiVO_4$

4.2.1 Generalities on doped-$BiVO_4$

Since the photocatalytic efficiency of pure bismuth vanadate is low and leads to reasonable photodegradation rates only after long irradiation time, modification of $BiVO_4$ is necessary. The development of modified $BiVO_4$ includes the increase of surface area, number of photocatalytic sites, number of absorbed photons, charge carrier separation and also the decrease in energy band gap E_g (Ibhadon and Fitzpatrick 2013). Doping is a technique commonly used to improve the photocatalytic performance of $BiVO_4$. The principle of this method is based on the insertion of electron donor or acceptor species (referred as n- and p-type dopants, respectively) in the crystalline structure of $BiVO_4$. As a result discrete electronic energy levels are inserted within the E_g of the semiconductor (**Fig. 6**). At optimal dopant concentration, an excess of hole and electron population is present in the VB and CB, respectively. The beneficial effects that are usually observed in a doped semiconductor photocatalyst are (1) reduction of E_g, (2) enhancement of electrical conductivity, (3) increase of e^-/h^+ pair separation and (4) improvement in surface adsorption of target molecule (Huang et al. 2014a).

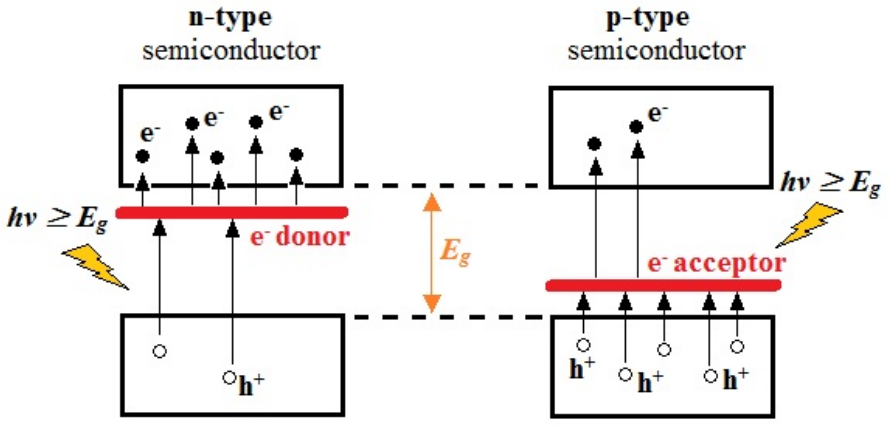

Fig. 6 Illustration of n- and p-type doping in a semiconductor

However the doping techniques should be distinguished from decoration and surface plasmon resonance (SPR) phenomena. Indeed, many researchers considered such methods as

doping (Long et al. 2011; Zhang et al. 2009; Zhang et al. 2018) but the principles of these techniques are different from those using “real” dopants (Obregon and Colon 2014; Shan and Liu 2016). For example, noble metals are often used to decorate $BiVO_4$ and they can trap photogenerated e^- (**Fig. 7**). Thus, e^-/h^+ separation is favored (Long et al. 2011; Zhang et al. 2009). On the other hand, noble metal nanoparticles can also shift the photoactivation of $BiVO_4$ toward longer wavelength due to SPR, and thus a transfer of electrons occurs from the decorating nanoparticle to the $BiVO_4$ CB as seen in **Fig. 7** (Long et al. 2011).

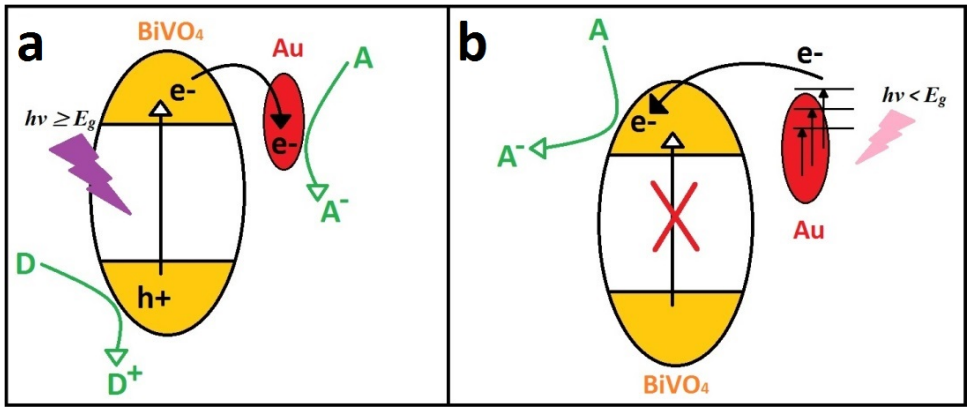

Fig. 7 Decorated $BiVO_4$ with Au nanoparticle. The different role of gold involved either in (a) electron trapping or (b) surface plasmon resonance. It is important to notice that these two processes occur under different irradiation energies i.e. wavelength (a) greater and (b) smaller than E_g

The use of metal and non-metal doping is not the easiest technique for improving the properties of a material. Indeed, to the determination of their optimal concentration, the dopants should be concentrated at the surface of the photocatalyst because they favor charge recombination in the material bulk. In the case of $BiVO_4$, which is a n-type semiconductor, tunsgten(VI) and molybdenium(VI) have been found to be the most promising n-type dopants among numerous transition and rare earth metals (Berglund et al. 2012; Huang et al. 2014a; Li et al. 2013a; Luo et al. 2011; Park et al. 2011; Park et al. 2013; Parmar et al. 2012; Ye et al. 2010). Mo(VI) and W(VI) improve the electronic properties of $BiVO_4$ (especially for water

oxidation) while other dopants such as Cu, Yb, Er, Nd and Sm ions are beneficial to the morphology and surface area of $BiVO_4$, but also to better visible light absorption associated with a decrease of E_g. **Table 2** summarises the effect of doped $BiVO_4$ on the efficiency of pollutant photodegradation. It is worth to notify that, in some works relatively, high amount of dopants is used (Huang et al. 2014b; Zhou et al. 2010). Therefore, the metal impurity is not inserted in $BiVO_4$ lattice, but it is surely present in another form such as a decorated oxide.

Table 2. Summary of photocatalytic degradation of different pollutants using doped $BiVO_4$.

Dopant	**Form**	**Pollutant**	**Irradiation**	**Photocatalytic efficiency (from "*pure*" to "*doped*")**	**Ref.**
Eu(III) + F	Powder (0.6 g/L)	RhB (10 mg/L)	Solar	From 65 to 100 % after 60 min	Xue et al. (2017)
Nd(III) + Er(III)	Powder (1 g/L)	RhB (10 mg/L)	Solar	From 57 to 96 % after 150 min	Liu et al. (2017)
0.01% Ag(I)	Powder (1 g/L)	MB (10 ppm)	Visible	From 55 to 100 % after 60 min	Huang et al. (2017)
10 at% Gd(III)	Powder (1 mg/L)	RhB (5 mg/L)	Solar	from 40 to 95 % after 120 min	Luo et al. (2016)
10 at% Nb(V)	Film (1.5 cm^2)	RhB (10^{-5} M)	Solar	From 51 to 72 % after 180 min	Monfort et al. (2017b)
2.5 mol% Fe(III)	Powder (1 g/L)	MB (20 mg/L)	Visible	From 25 to 55 % after 180 min	Chala et al. (2014)
6 at% Sm(III)	Powder (1 g/L)	RhB (5 mg/L)	Solar	from 40 to 95 % after 120 min	Luo et al. (2015a)
10 at% Nd(III)	Powder (1 g/L)	RhB (5 mg/L)	Solar	from 40 to 95 % after 120 min	Luo et al. (2015b)
Er(III) + Yb(III)	Powder	RhB (20 mg/L)	Infra-Red	Until 25 % after 180 min	Shan and Liu (2016)
8 at% Yb(III)	Powder (1 g/L)	RhB (5 mg/L)	Solar	from 50 to 95 % after 120 min	Huang et al.

					(2014b)
0.75 at% Er(III)	Powder (1 g/L)	MB (10 mg/L)	Solar	from 65 to 100 % after 40 min	Obregon and Colon (2014)
0.75 wt% Cu(II)	Powder (1 mg/L)	Phenol (10 mg/L)	Visible	from 55 to 90 % after 180 min	Gao et al. (2015)
4 mol% B	Powder (0.2 g/L)	MO (15 mg/L)	Visible	from 30 to 95 % after 50 min	Wang et al. (2015)
3 mol% N	Powder (1 mg/L)	RhB ($2 \cdot 10^{-5}$ M)	Solar	from 50 to 100 % after 240 min	Tan et al. (2014)
5 mol% PO_4^{3-}	Powder (1 g/L)	MB (10 mg/L)	Solar	From 55 to 90 % after 300 min	Liu et al. (2016)
6 mol% Co(II)	Powder (0.6 g/L)	MB (10 mg/L)	Visible	From 68 to 93 % after 300 min	Geng et al. (2015)
5 wt% Co(II)	Powder (1 g/L)	MB (15 mg/L)	Visible	From 65 to 80 % after 330 min	Zhou et al. (2010)
1.5 mol% Cu(II)	Powder (0.6 g/L)	RhB (15 mg/L)	Visible	From 46 to 95 % after 50 min	Wang et al. (2017a)
Ni(II) + B	Powder (0.2 g/L)	MO (15 mg/L)	Visible	From 25 to 95 % after 50 min	Wang et al. (2017b)
1 wt% Fe(III)	Powder (1.4 g/L)	Ibuprofen (20 mg/L)	Visible	From 35 to 70 % after 60 min	Regmi et al. (2017)

RhB = rhodamine B; MB = methylene blue; MO = methyl orange

4.2.2 Efficiency of doped-$BiVO_4$

The efficiency of doped-$BiVO_4$ photocatalyst compared to pure $BiVO_4$ is undoubtedly better due to the different reasons discussed just above. However, since the photocatalytic properties are often tested for the degradation of an organic dye (**Table 2**), the real efficiency of the modified photocatalyst is disputable. Indeed, most of the works only follow the decolorisation process (refs. in **Table 2**). By this way, only the degradation of the

chromophore function is proved, but no information about the mineralisation of the entire molecule is given. Fortunately, some works are devoted to the real degradation efficiency using doped photocatalyst, especially Regmi et. al (2017) whom followed by HPLC the degradation process of ibuprofen using Fe-doped $BiVO_4$. They discussed the gradual degradation of this pharmaceutical into the formation of by-products that are themselves also degraded until the mineralisation (Regmi et. al 2017). The degradation process is discussed in details: the first step of photooxidation is a multi-hydroxylation of the pollutant followed by a cycle-opening until the oxidation into ketones and carboxylic acids before full mineralisation into CO_2 and H_2O (Regmi et. al 2017). Zhang et. al (2018) also discussed the photooxidative properties of Co/Pd-$BiVO_4$ for phenol removal by supporting on HPLC results while Luo et. al (2016) discussed the efficiency of Gd-doped $BiVO_4$ by using TOC analysis. The TOC removal is measured to be only 15% while the decolorisation rate reaches 95% indicating that the mineralisation degree in the removal of an organic dye is very low (Luo et. al 2016). Therefore, all the works focused on photocatalytic properties using an organic dye as model pollutant should be interpreted with caution.

On the other hand, the reproducibility of photocatalytic measurements and the reusability of photocatalysts are also crucial parameters in the efficiency of photodegradation processes since they can be considered as limiting factors. With this respect, the use of photocatalytic layer is better than powder suspension system for practical reasons. Many researchers have studied the reusability of modified $BiVO_4$ (refs. in **Table 2**), which generally shows an excellent reproducibility in pollutant degradation. This characteristic should be always tested since some materials cannot be reused as for example Nb-$BiVO_4$ (Monfort et al. 2017b). Indeed, such a photocatalyst exhibits excellent photooxidative properties in the degradation of Rhodamine B (Monfort et al. 2017b), but after repeated use, the photocatalytic efficiency decreases and it is even worse than pure $BiVO_4$, which has good stability over time

(**Fig. 8**). This observation is probably due to by-products obstruction in the porous and hierarchical structure of Nb-$BiVO_4$ material since the degradation of organic dye is not complete (Luo et al. 2016; Monfort et al. 2017b).

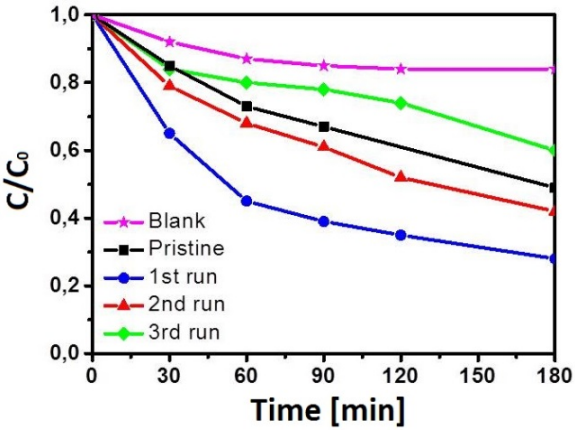

Fig. 8 Reproducibility of Rhodamine B photodegradation using Nb-$BiVO_4$ under solar light (under identical experimental conditions as in Monfort et al. 2017b)

4.2.3 Mechanism using doped-$BiVO_4$

The photooxidative degradation mechanism of organic pollutants could show differences between various doped-$BiVO_4$ due to the wide range of tested dopants. Thus, it is extremely important to study deeply and experimentally the photodegradation mechanism for a better understanding of each doped system. Charge scavenger technique and photoluminescence spectroscopy are generally used to detect the formation (or not) of oxidative radical species, but most of the works base their discussion on calculations and theory which are often not correlated by the experiments (refs. in **Table 2**). For Cu-doped $BiVO_4$, Gao et. al (2015) have found that the main oxidative species are the hydroxyl radicals ($OH^{\bullet}$) and holes while $O_2^{\bullet-}$ play a minor role. This is due to copper that acts as electron scavenger; thus it increases the e^-/h^+ pair separation and consequently the photocatalytic efficiency. On the other hand, Xue et. al (2017) have studied the photocatalytic properties of

Eu- and F-codoped $BiVO_4$. They have found that the main oxidation species in the degradation of Rhodamine B are superoxide radicals since almost no effect is observed in the presence of holes and $OH^{\bullet}$ scavengers. In this case, they ascribe the excellent photocatalytic properties of doped $BiVO_4$ to Eu(III) which plays the role of e^- trap for efficient formation of $O_2^{\bullet-}$ (Xue et. al 2017). In addition, Xue et. al (2017) ascribe also to Eu and F dopants the better crystallinity and morphology of the photocatalyst (compared to bare $BiVO_4$). Another example of mechanism using doped $BiVO_4$ is Co/Pd-decorated bismuth vanadate (Zhang et. al 2018). In their work, Zhang et. al (2018) have shown that the main oxidative species in phenol degradation are holes and $O_2^{\bullet-}$ using both charge scavenger and EPR. They explain the observed mechanism by Co/Pd which traps e^-. Therefore, it enhances the formation of $O_2^{\bullet-}$ while h^+ can oxidise directly phenol since the redox potential for $OH^{\bullet}$ formation is not reached. These few examples show that the mechanism varies from one dopant to another, but it shows also that degradation mechanism is not clearly determined since different authors have identified different oxidative species for a given doped material (refs. in **Table 2**). Therefore, studies on mechanism should be deepened because it is a necessary knowledge for the development of doped-$BiVO_4$ systems in potential environmental applications.

4.3 $BiVO_4$ composites

4.3.1 Generalities on $BiVO_4$ composites

The elaboration of composite is also an efficient way to improve the photocatalytic properties of $BiVO_4$ (Gholipour et al. 2015). Usually, a semiconductor photocatalyst like bismuth vanadate can be assembled with several types of materials such as another semiconductor or a metal to form a heterojunction or a decorated photocatalyst, respectively, or $BiVO_4$ can even be assembled with carbon materials (carbon nanotube, graphene oxide,

etc.) (Gholipour et al. 2015; Huang et al. 2014a; Moniz et al. 2015; Park et al. 2013 ; Xu et al. 2014 ; Zhang et al. 2012 ; Zhu et al. 2017a). In this section, we will focus on semiconductor heterojunctions which are of three types defined according to their electronic band structure (**Fig. 9**) (Gholipour et al. 2015; Huang et al. 2014a; Moniz et al. 2015).

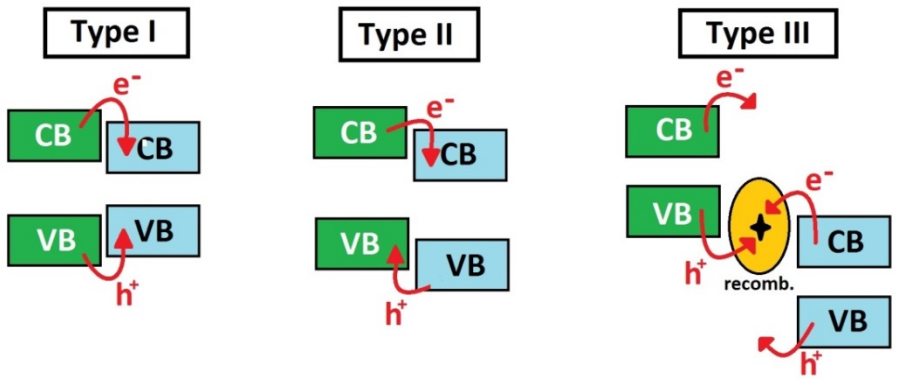

Fig. 9 Illustration of the 3 different types of semiconductor heterojunction

In type I, both photogenerated e^- and h^+ are transferred from semiconductor 1 (SC1) to semiconductor 2 (SC2) due to position of E_{g2}, which is within the E_{g1} (Gholipour et al. 2015). This kind of heterojunction does not improve the photocatalyst since all the charge carriers are transferred and accumulated in one semiconductor (Gholipour et al. 2015). In type II heterojunction, the VBM and CBM of semiconductor 1 are lower in energy than those of semiconductor 2, respectively (Gholipour et al. 2015; Huang et al. 2014a; Moniz et al. 2015; Park et al. 2013). As a result, the photogenerated e^- move from SC1 to SC2 while photogenerated h^+ migrate from SC2 to SC1 (Gholipour et al. 2015; Huang et al. 2014a; Moniz et al. 2015; Park et al. 2013). If both semiconductors are in sufficient contact, efficient charge carrier separation occurs during the photoactivation process (Gholipour et al. 2015; Huang et al. 2014a; Moniz et al. 2015; Park et al. 2013). Finally, the type III heterojunction consists of SC1 which has E_{g1} position higher in energy than E_{g2} of SC2. Consequently, recombination between h^+ from VB of SC1 and e^- from CB of SC2 occurs (Gholipour et al.

2015). This type of heterojunction could be interesting for designing indirect Z-scheme system with an appropriate electron mediator (Gholipour et al. 2015). In the rest of this section, we will discuss type II semiconductor heterojunction since it is the simplest way to limit e^-/h^+ pair recombination i. e. to improve charge carriers lifetime, to reach efficient charge transport and to enhance light absorption (Gholipour et al. 2015; Park et al. 2013).

Concerning $BiVO_4$, one of the most frequently used semiconductor for type II heterojunction is WO_3 (E_g = 2.6 eV) mainly for the purpose of water splitting (Chatchai et al. 2013; Fujimoto et al. 2014; Huang et al. 2014a; Moniz et al. 2015; Park et al. 2013; Pilosh et al. 2014). Another interesting composite is $BiVO_4/TiO_2$, which is also a type II semiconductor heterojunction with similar electronic band configuration to $BiVO_4/WO_3$. However, one could say that the E_g of TiO_2 should energetically encompass the E_g of $BiVO_4$ to form a type I heterojunction since CBM of TiO_2 and $BiVO_4$ is -0.2 V and 0 V, respectively, while VBM is at 3.0 V and 2.4 V for TiO_2 and $BiVO_4$, respectively (Guo et al. 2016; Hu et al. 2011; Sun et al. 2015). But this is only valid for the single components (Guo et al. 2016; Hu et al. 2011; Sun et al. 2015). Indeed, in the heterojunction, the energy band gap position of $BiVO_4$ and TiO_2 is shifted by homogenisation of their Fermi levels (Guo et al. 2016; Hu et al. 2011; Sun et al. 2015). Therefore, after the thermodynamical equilibrium in $BiVO_4/TiO_2$, the VBM and CBM of $BiVO_4$ are lower in energy than those of TiO_2, respectively (Guo et al. 2016; Hu et al. 2011; Sun et al. 2015). This is an important feature of the heterojunction that should be taken into consideration for discussing the real charge transfer in a composite. The **Table 3** summarises various $BiVO_4$ composites for pollutant photodegradation. In addition, **Fig. 10** illustrates the energetic positions of CBM and VBM of the semiconductor components in different heterojunctions calculated from the Mulliken electronegativity theory (**eqs. 10 - 12**). This theory does not take into account the thermodynamical equilibrium of the Fermi level in

the heterojunction, but the **Fig. 10** gives an overview of the possibility of designing semiconductor heterojunction photocatalyst with $BiVO_4$.

$$E_{CB} = X - E^e - 0.5E_g \quad (10)$$

$$E_{VB} = E_g + E_{CB} \quad (11)$$

$$X = [\chi(A)^a \chi(B)^b \chi(C)^c]^{1/(a+b+c)} \quad (12)$$

where E_{VB} and E_{CB} are the VB and CB edge potentials, X is the absolute electronegativity of the semiconductor (a, b and c are the atomic number of the compounds A, B and C respectively), E_g is the energy band gap of the semiconductor and E^e is the energy of free electrons on the hydrogen scale (4.5 eV).

Table 3. Summary of photocatalytic degradation of different pollutants using $BiVO_4$ composite.

Composite with	**Form**	**Pollutant**	**Irradiation**	**Photocatalytic efficiency (from "*pure*" to "*composite*")**	**Ref.**
TiO_2	Powder (1.35 g)	Benzene (20 mL/min)	Visible	from 5 to 60 % after 8 h	Hu et al. (2011)
TiO_2	Powder (20 mg)	Toluene (4 µL)	Visible	from 55 to 90 % after 6 h	Sun et al. (2015)
CuO_x	Powder (unknown quantity)	Bisphenol A (210 µg/L)	Solar	Until 90 % after 120 min	Kanigaridou et al. (2016)
$InVO_4$	Film (3 layers)	MB (10^{-5} M)	Visible	from 35 to 70 % after 120 min	Lamdab et al. (2016)
Ag/Ag_2CO_3	Powder (0.4 g/L)	Tetracycline (20 mg/L)	Visible	from 47 to 95 % after 150 min	Liu et al. (2018)
$FeVO_4$	Powder (4 g/L)	Metronidazole (10 mg/L)	Visible	from 40 to 90 % after 90 min	Li et al. (2015)
$Ag_4V_2O_7$	Powder (1 g/L)	MB (5 mg/L)	Visible	From 30 to 100 % after 60 min	Hu et al. (2017)
Fe_3O_4	Powder (3 g/L)	Acid Red B	Visible	Until 98 % after 120 min	Zhai et al. (2017)

		(20 mg/L)			
TiO_2	Powder (0.5 g/L)	RhB (10 mg/L)	Visible	from 10 to 90 % after 240 min	Guo et al. (2016)
TiO_2	Film (1.5 cm²)	RhB B (10^{-5} M)	Solar	from 50 to 61 % after 180 min	Monfort et al. (2017a)
TiO_2	Film (100 mg)	MB ($5{\cdot}10^{-5}$ M)	Visible	from 69 to 88 % after 120 min	Pingmuang et al. (2014)
TiO_2	Powder (1 g/L)	MB ($2{\cdot}10^{-5}$ M)	Solar	from 45 to 84 % after 120 min	Wetchakun et al. (2015)
$SrTiO_3$	Powder (1 g/L)	Sulfamethoxazole (10 mg/L)	Solar	from 50 to 90 % after 60 min	Li et al. (2017)
TiO_2	Film (1.6 cm²)	Rh6G ($6{\cdot}10^{-6}$ M)	Visible	Until 70 % after 300 min	Odling and Robertson (2016)
Ag_3PO_4	Powder (0.5 g/L)	MB (10 mg/L)	Visible	from 50 to 100 % after 10 min	Li et al. (2013c)
Bi_2WO_6	Powder (1 g/L)	RhB ($5{\cdot}10^{-5}$ M)	Visible	from 50 to 90 % after 30 min	Ju et al. (2014)
Ag_2O	Powder (1 g/L)	MO (5 mg/L)	Solar	from 36 to 47 % after 180 min	Shan et al. (2014)
CdS	Powder (0.6 g/L)	MG (15 mg/L)	Visible	from 20 to 95 % after 120 min	Fang et al. (2016)
BiOBr	Powder (1 g/L)	RhB (10^{-5} M)	Visible	from 55 to 97 % after 100 min	Yuan et al. (2016)
MnO_2 + Au	Film (1.5 cm²)	MB (10^{-5} M)	Solar	Until 76 % after 150 min	Trzcinski et al. (2016)
WO_3	Powder (1.25 g/L)	2-chlorophenol (0.3 mM)	Visible	Until 92 % after 180 min	Selvarajan et al. (2017)
TiO_2	Powder (1.25 g/L)	Phenol (20 mg/L)	Visible	From 10 to 75 % after 100 min	Zhu et al. (2017b)
TiO_2	Film	Ethylene (0.15 mg/L)	Visible	Until 8 % after 360 min	Song et al. (2017)
Cu_2O	Powder (0.5 g/L)	MB ($2{\cdot}10^{-5}$ M)	Visible	From 80 to 100 % after 90 min	Yuan et al. (2014)
$ZnFe_2O_4$	Powder (2 g/L)	MB (15 mg/L)	Visible	From 70 to 100 % after 300 min	Xu and Song (2017)
$Bi_2Ti_2O_7$	Powder (1 g/L)	Tetracycline (10 mg/L)	Solar	From 50 to 100 % after 60 min	Li et al. (2016b)

MG = Methylene Green; Rh6G = Rhodamine 6G, MO = Methyl Orange

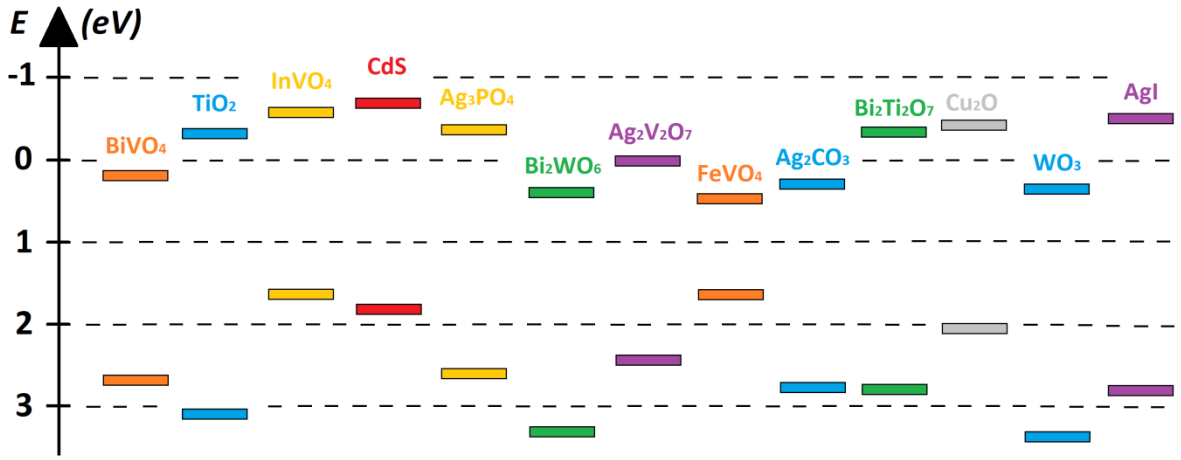

Fig. 10 Energetic position of the VBM and CBM calculated from Mulliken electronegativity theory in different heterojunction materials (refs. in Table 3)

4.3.2 Efficiency of $BiVO_4$ composites

It can be seen from **Table 3** that the use of composite systems increase the photocatalytic efficiency by more than a factor 2 compared to bare $BiVO_4$. However, the recurrent problem in photocatalytic study is that only the initial concentration of the target pollutant is followed. Thus few of the reported works in **Table 3** focuses on the real efficiency in full mineralisation of organic pollutants. For instance, in gas system such as benzene and toluene, the analysis of efficiency is relatively simple since a gas chromatograph is necessary. In water matrix, Kanigaridou et. al (2016) have identified by liquid chromatography-mass spectroscopy the by-products from the degradation of bisphenol A. Using $CuO_x/BiVO_4$, hydroxylation of bisphenol A occurs until the scission of the molecule and subsequently to ring-opening until mineralisation is reached (Kanigaridou et al. 2016). On the other hand, Li et. al (2016b) have identified the by-products from the photooxidation of a pharmaceutical (tetracycline) in presence of $Bi_2Ti_2O_7/BiVO_4$ using HPLC. However, further studies on open-ring molecules have not been performed. Similarly, Liu et. al (2018) have used HPLC and GC-MS to study the efficiency in the degradation of tetracycline using $Ag/Ag_2CO_3/BiVO_4$

composite photocatalyst. They have found out that tetracycline is degraded by successive oxidations resulting in open-ring molecule, and finally mineralisation into CO_2, H_2O and NH_4^+ is reached (Liu et al. 2018). In light of the small amount of works focused on the real efficiency of $BiVO_4$ composites, supplementary studies are necessary to deepen the knowledge to a wide range a pollutants.

In addition, the reproducibility in pollutant degradation using regenerated photocatalyst is often a limiting factor for heterogeneous photocatalytic process. In the case of the composites containing $BiVO_4$ (refs. in **Table 3**), most of the photocatalysts exhibit excellent reproducibility in photocatalytic process and can be reuse without significant changes in the degradation rate until 5 times. Before reusing the photocatalyst, the photoactive material should be regenerated by cleaning process followed by reannealing.

4.3.3 Mechanism using $BiVO_4$ composites

Different mechanisms could be observed according to the nature of the semiconductor associated with $BiVO_4$. Therefore, it is crucial to investigate experimentally the mechanism of photodegradation for a given composite system. For example, Kanigaridou et. al (2016) have detected hydroxyl radicals using EPR measurements for the degradation of bisphenol A in presence of $CuO_x/BiVO_4$ composite, but they do not detailed the electronic band structure of the photocatalyst. Similarly, Yuan et. al (2014) have found by photoluminescence measurements that $OH^{\bullet}$ radicals are probably the main oxidising species in the degradation of an organic dye using $Cu_2O/BiVO_4$. In many works (**Table 3**), the mechanism of photooxidative degradation is often determined using charge scavengers, photoluminescence and calculations using Mullinken electronegativity. By this way, the corresponding band structure of the composite can be determined. However some of the works reported in **Table**

3 only focuses on the detection of hydroxyl radicals. Therefore, a large gap in mechanism discussion is left and the rest of the mechanism is explained based on the theory.

Various photooxidative mechanisms have been identified using different composites. For instance, Li et. al (2015) have found that the main oxidising species in the degradation of metronidazole using $FeVO_4/BiVO_4$ are $O_2^{\bullet-}$ while for $Ag_4V_2O_7/BiVO_4$ and $Bi_2Ti_2O_7/BiVO_4$, the main oxidative species in the degradation of MB and tetracycline, respectively, are hydroxyl radicals (Hu et al. 2017; Li et al. 2016b). Another example, Liu et al. (2018) have studied the mechanism of tetracycline using $Ag/Ag_2CO_3/BiVO_4$ and they have found that $OH^{\bullet}$ and h^+ are the main oxidising species. Atypical systems have the advantages to be decorated such as $Ag/Ag_2CO_3/BiVO_4$ (by silver), $BiVO_4/Ag_2O$ and $BiVO_4/Fe_3O_4$, where the decorated compounds play a role of e^- trap (refs. in **Table 3**). Therefore, the lifetime of e^-/h^+ pair increases. The explanation of the differences between mechanisms is due to the relative position of E_g of the components in the composite. Indeed, the band structure of the heterojunction governs the charge transfer within the composite, where accumulation of e^- in CB of $BiVO_4$ and h^+ in VB of the other side is often observed (refs. in **Table 3**). In addition, after the thermodynamical equilibrium of Fermi level, the redox potentials of VBM and CBM differs according to the nature of the component associated with $BiVO_4$. Finally, other phenomena can influence the mechanism such as sensitisation, surface plasmon resonance and adsorption (refs. in **Table 3**). Therefore the existing and actual studies on mechanism using $BiVO_4$-based composites should be taken with caution.

A particular attention is given to $TiO_2/BiVO_4$ system since many works are devoted to this composite. By reporting to other works, the mechanism of photooxidative reactions using $BiVO_4/TiO_2$ composite is still a matter of discussion due to incomplete or lack of experimental data. Indeed, even if the experimental and theoretical methods used in these studies often lead to a type II $BiVO_4/TiO_2$ heterojunction, the reported energy level of E_g and

the identity of oxidative species are different from one work to another, suggesting that additional work is needed (refs. in **Table 3**). Many authors describe a photooxidation process but through different radicals as main oxidising species, either $O_2^{\bullet-}$ or $OH^{\bullet}$ or even h^+ (Guo et al. 2016; Hu et al. 2017; Sun et al. 2015; Wetchakun et al. 2015), while Odling et. al (2016) preconised a sensitisation of the photocatalyst when a dye is the targeted pollutant. Finally, Monfort et. al (2017a) have studied the mechanism of dye degradation using different layered $BiVO_4/TiO_2$ composites. Such a layered system is considerably different from powder suspension and the photocatalytic properties are probably more interesting to investigate. In this study, they notice that the top-coated layer of the composite has an influence on the photocatalytic mechanism since the interface could be different in respect with the layer configuration i.e. the nature of semiconductor at the surface of the composite (Monfort et. al 2017a). Indeed, the photooxidative degradation of rhodamine B under solar irradiation runs through h^+ for top-coated $BiVO_4$ (on TiO_2) while $O_2^{\bullet-}$ is identified as main oxidative species for top-coated TiO_2 (on $BiVO_4$) (Monfort et. al 2017a). All these different results on $TiO_2/BiVO_4$ but also on the other $BiVO_4$ composite systems exhibit that deepened studies are needed to really understand the mechanism of photooxidative process which is not trivial.

5 Summary and perspectives

This short review summarised the most important results collected using $BiVO_4$-based photocatalysts. Bismuth vanadate is a semiconductor that gains stronger interest in the photochemical community since the number of publications devoted to photocatalytic systems composed of $BiVO_4$ increases promptly. However, many uncertainties about the photocatalytic efficiency and mechanism have been highlighted in this critical review. This issue reflects the quick increase of interest for this promising material where researchers

attempt to present new insights of $BiVO_4$-based photocatalysts rather than to focus on deepened study. Therefore, such a photocatalyst cannot be actually implemented in environmental applications although $BiVO_4$ is highly promising.

Indeed, $BiVO_4$-based photocatalyst can be activated under solar light; thus designed in the form of film, which presents many advantages compared to powder systems, sunlight-driven bismuth vanadate materials can be deposited on foams or membranes for simultaneous filtration and degradation of pollutants in air and surface water. Such a material, which can be also used as electrode in water splitting processes as well as solar cells, would gain in popularity, especially for the design of pilot scale test, if the knowledge on $BiVO_4$-based systems is deepened.

References

An T, An J, Yang H et al. (2011) Photocatalytic degradation kinetics and mechanism of antivirus drug-lamivudine in TiO2 dispersion. J Hazard Mater 197:229-236

Azenha E, Romeiro A, Sarakha M (2013) Photodegradation of Pesticides and Photocatalysis in the Treatment of Water and Waste. In: Evans RC, Douglas P, Burrows HD (Eds.) Applied Photochemistry. Springer, Dordrecht, pp 247-266

Berglund SP, Rettie AJE, Hoang S et al. (2012) Incorporation of Mo and W into nanostructured BiVO4 films for efficient photoelectrochemical water oxidation. Phys Chem Chem Phys 14:7065-7075

Bhat SSM and Jang HW (2017) Recent Advances in Bismuth-Based Nanomaterials for Photoelectrochemical Water Splitting. ChemSusChem 10:3001-3018

Chala S, Wetchakun K, Phanichphant S et al. (2014) Enhanced visible-light-response photocatalytic degradation of methylene blue on Fe-loaded BiVO4 photocatalyst. J Alloy Compd 597:129-135

Chatchai P, Nosaka AY, Nosaka Y (2013) Photoelectrocatalytic performance of WO3/BiVO4 toward the dye degradation. Electrochim Acta 94:314-319

Chen Y, Hu C, Qu J et al. (2008) Photodegradation of tetracycline and formation of reactive oxygen species in aqueous tetracycline solution under simulated sunlight irradiation. J Photochem Photobio A 197:81-87

Chen X, Shen S, Guo L et al. (2010) Semiconductor based Photocatalytic Hydrogen Generation. Chem Rev 110:6503-6570

Chen L, Wang J, Meng D et al. (2016) The pH-controlled (040) facets orientation of BiVO4 photocatalysts with different morphologies for enhanced visible light photocatalytic performance. Mater Lett 162:150-153

Chiarello GL and Selli E (2010) Photocatalytic Hydrogen Production. Recent Pat Eng 4(3):155-169

Edge R (2013) Radiolytic and Photolytic production of Free Radicals and Reactive Oxygen Species: Interactions with Antioxidants and Biomolecules. In: Evans RC, Douglas P, Burrows HD (Eds.) Applied Photochemistry. Springer, Dordrecht, pp 305-330

Fan H, Wang D, Wang L et al. (2011) Hydrothermal synthesis and photoelectric properties of BiVO4 with different morphologies: An efficient visible-light photocatalyst. Appl Surf Sci 257:7758-7762

Fan H, Jiang T, Li H et al. (2012) Effect of BiVO4 Crystalline Phases on the Photoinduced Carriers Behavior and Photocatalytic Activity. J Phys Chem C 116:2425-2430

Fang GD, Dionysiou DD, Zhou DM et al. (2013) Transformation of polychlorinated biphenyls by persulfate at ambient temperature. Chemosphere 90:1573-1580

Fang S, Xue S, Wang C et al. (2016) Fabrication and characterization of CdS/BiVO4 nanocomposites with efficient visible light driven photocatalytic activities. Ceram Int 42:4421-4428

Fujimoto I, Wang N, Saito R et al. (2014) WO3/BiVO4 composite photoelectrode prepared by improved auto-combustion method for highly efficient water splitting. Int J Hydrogen Energ 39(6):2454-2461

Galembeck A and Alves OL (2000) BiVO4 thin film preparation by metalorganic decomposition. Thin Solid Films 365:90-93

Gan J, Lu X, Tong Y (2014) Towards highly efficient photoanodes: boosting sunlight-driven semiconductor nanomaterials for water oxidation. Nanoscale 6:7142-7164

Gao X, Wang Z, Fu F et al. (2015) Effects of pH on the hierarchical structures and photocatalytic performance of Cu-doped BiVO4 prepared via hydrothermal method. Mat Sci Semicon Proc 35:197-206

Garcia-Perez UM, Sepulveda-Guzman S, Martinez-de la Cruz A et al. (2012) Selective Synthesis of Monoclinic Bismuth Vanadate Powders by Surfactant-Assisted Co-Precipitation Method: Study of Their Electrochemical and Photocatalytic Properties. Int J Electrochem Sci 7:9622-9632

Gaya UI (2014) Heterogeneous Photocatalysis Using Inorganic Semiconductor Solids. Springer, Dordrecht

Geng Y, Zhang P, Li N et al. (2015) Synthesis of Co doped BiVO4 with enhanced visible-light photocatalytic activities. J Alloy Compd 651:744-748

Gholipour MR, Dinh CT, Beland F et al.(2015) Nanocomposite heterojunctions as sunlight-driven photocatalysts for hydrogen production from water splitting. Nanoscale 7:8187-8208

Guo Y, Yang X, Ma F et al. (2010) Additive-free controllable fabrication of bismuth vanadates and their photocatalytic activity toward dye degradation. Appl Surf Sci 256:2215-2222

Guo Z, Li P, Che H et al. (2016) One-dimensional spindle-like BiVO4/TiO2 nanofibers heterojunction nanocomposites with enhanced visible light photocatalytic properties. Ceram Int 42:4517-4525

Hashimoto K, Irie H, Fujishima A (2005) TiO2 Photocatalysis: A Historical Overview and Future Prospects. Jpn J Appl Phys 44(12):8269-8285

Herrmann JM (1999) Heterogeneous photocatalysis: fundamentals and applications to the removal of various types of aqueous pollutants. Catal Today 53:115-129

Hinojosa-Reyes L, Guzman-Mar JL, Villanueva-Rodriguez M (2015) Semiconductor Materials for Photocatalytic Oxidation of Organic Pollutants in Wastewater. In: Hernandez-Ramirez A, Medina-Ramirez I (Eds.) Photocatalytic Semiconductors. Springer, Cham, pp 187-228

Hofmann M, Rainer M, Schulze S et al. (2015) Nonaqueous Synthesis of a Bismuth Vanadate Photocatalyst By Using Microwave Heating: Photooxidation versus Photosensitized Decomposition in Visible-Light-Driven Photocatalysis. ChemCatChem 7:1357-1365

Hu L, Flanders PM, Miller PL et al. (2007) Oxidation of sulfamethoxazole and related antimicrobial agents by TiO2 photocatalysis. Water Res 41:2612-2626

Hu Y, Li D, Zheng Y et al. (2011) BiVO4/TiO2 nanocrystalline heterostructure: A wide spectrum responsive photocatalyst towards the highly efficient decomposition of gaseous benzene. Appl Catal B 104:30-36

Hu Y, Li D, Sun F et al. (2015) One-pot template-free synthesis of heterophase BiVO4 microspheres with enhanced photocatalytic activity. RSC Adv 5:54882-54889

Hu Y, Fan J, Pu C et al. (2017) Facile synthesis of double cone-shaped Ag4V2O7/BiVO4 nanocomposites with enhanced visible light photocatalytic activity for environmental purification. J Photochem Photobiol A 337:172-183

Huang ZF, Pan L, Zou JJ et al. (2014a) Nanostructured Bismuth Vanadate-Based Materials for Solar-Energy-Driven Water Oxidation: A Review on Recent Progress. Nanoscale 6:14044-14063

Huang J, Tan G, Zhang L et al. (2014b) Enhanced photocatalytic activity of tetragonal BiVO4: Influenced by rare earth ion Yb3+. Mater Lett 133:20-23

Huang CK, Wu T, Huang CW et al. (2017) Enhanced photocatalytic performance of BiVO4 in aqueous AgNO3 solution under visible light irradiation. Appl Surf Sci 399:10-19

Hubert-Pfalzgraf LG (2003) Some trends in the design of homo- and heterometallic molecular precursors of high-tech oxides. Inorg Chem Commun 6:102-120

Ibhadon AO and Fitzpatrick P (2013) Heterogeneous Photocatalysis: Recent Advances and Applications. Catalysts 3:189-218

Jiang H, Dai H, Meng X et al. (2011) Porous olive-like BiVO4: Alcoho-hydrothermal preparation and excellent visible-light-driven photocatalytic performance for the degradation of phenol. Appl Catal B 105:326-334

Jiang H, Dai H, Meng X et al. (2012) Hydrothermal fabrication and visible-light-driven photocatalytic properties of bismuth vanadate with multiple morphologies and/or porous structures for Methyl Orange degradation. J Environ Sci 24(3):449-457

Ju P, Wang P, Li B et al. (2014) A novel calcined Bi2WO6/BiVO4 heterojunction photocatalyst with highly enhanced photocatalytic activity. Chem Eng J 236:430-437

Kanigaridou Y, Petala A, Frontistis Z et al. (2016) Solar photocatalytic degradation pf bisphenol A with CuOx/BiVO4: Insights into the unexpectedly favorable effect of bicarbonates. Chem Eng J 318:39-49

Katsumata H, Taniguchi M, Kaneco S. et al. (2013) Photocatalytic degradation of bisphenol A by Ag3PO4 under visible light. Catal Commun 34:30-34

Ke D, Peng T, Ma L et al. (2008) Photocatalytic water splitting for O2 production under visible-light irradiation on BiVO4 nanoparticles in different sacrificial reagent solutions. Appl Catal A 350:111-117

Koltsakidou A, Antonopoulou M, Evgenidou E et al. (2017) Cytarabine degradation by simulated solar assisted photocatalysis using TiO2. Chem Eng J 316:823-831.

Kumar KV, Porkodi K, Rocha F (2008) Langmuir-Hinshelwood kinetics - A theoretical study. Catal Commun 9(1):82-84

Larsson DGJ (2014) Pollution from drug manufacturing: review and perspectives. Philos T Roy Soc B 369:71-78

Lamdab U, Wetchakun K, Phanichphant S et al. (2016) InVO4-BiVO4 composite films with enhanced visible light performance for photodegradation of methylene blue. Catal Today 278(2):291-302

Lazar MA, Varghese S, Nair SS (2012) Photocatalytic Water Treatment by Titanium Dioxide: Recent Updates. Catalysts 2:572-601

Lelario F, Brienza M, Bufo SA et al. (2016) Effectiveness of different advanced oxidation processes (AOPs) on the abatement of the model compound mepanipyrim in water. J Photochem Photobiol A 321:187-201

Li G, Zhang D, Yu JC (2008) Ordered Mesoporous BiVO4 through Nanocasting: A Superior Visible Light-Driven Photocatalyst. Chem Mater 20(12):3983-3992

Li Z, Luo W, Zhang M et al. (2013a) Photoelectrochemical cells for solar hydrogen production: current state of promising photoelectrodes, methods to improve their properties, and outlook. Energ Environ Sci 6:347-370

Li R, Zhang F, Wang D et al. (2013b) Spatial separation of photogenerated electrons and holes among {010} and {110} crystal facets of BiVO4. Nat Commun 4:1432-1439

Li C, Zhang P, Lv R et al. (2013c) Selective Deposition of Ag3PO4 on Monoclinic BiVO4 (040) for Highly Efficient Photocatalysis. Small 9(23):3951-3956

Li J, Zhao W, Guo Y et al. (2015) Facile synthesis and high activity of novel BiVO4/FeVO4 heterojunction photocatalyst for degradation of metronidazole. Appl Surf Sci 351:270-279

Li F, Kang Y, Chen M et al. (2016a) Photocatalytic degradation and removal mechanism of ibuprofen via monoclinic BiVO4 under simulated solar light. Chemosphere 150:139-144

Li J, Han M, Guo Y et al. (2016b) Hydrothermal synthesis of novel flower-like BiVO4/Bi2Ti2O7 with superior photocatalytic activity toward tetracycline removal. Appl Catal A 524:105-114

Li J, Wang F, Meng L et al. (2017) Controlled synthesis of BiVO4/SrTiO3 composite with enhanced sunlight-driven photofunctions for sulfamethoxazole removal. J Colloid Interf Sci 485:116-122

Lianos P (2017) Review of recent trends in photoelectrocatalytic conversion of solar energy to electricity and hydrogen. Appl Catal B 210:235-254

Liao CH, Huang CW, Wu JCC (2012) Hydrogen Production from Semiconductor-based Photocatalysis via Water Splitting. Catalysts 2:490-516

Lin Y, Li D, Hu J et al. (2012) Highly Efficient Photocatalytic Degradation of Organic Pollutants by PANI-Modified TiO2 Composite. J Phys Chem C 116:5764-5772

Linsebigler AL, Lu G, Yates JTJ (1995) Photocatalysis on TiO2 Surfaces: Principles, Mechanisms, and Selected Results. Chem Rev 95:735-758

Litter MI (1999) Heterogeneous photocatalysis: Transition metal ions in photocatalytic systems. Appl Catal B 23:89-114

Liu W, Zhao G, An M et al. (2015) Solvothermal synthesis of nanostructured BiVO4 with highly exposed (010) facets and enhanced sunlight-driven photocatalytic properties. Appl Surf Sci 357:1053-1063

Liu W, Zhao G, Zhang Y et al. (2016) Hydrothermal synthesis of phosphate-doped BiVO4 with exposed (010) facets and enhanced sunlight-driven photocatalytic properties. Mater Lett 170:183-186

Liu T, Tan G, Zhao C et al. (2017) Enhanced photocatalytic mechanism of the Nd-Er co-doped tetragonal BiVO4 photocatalysts. Appl Catal B 213:87-96

Liu Y, Kong J, Yuan J et al. (2018) Enhanced photocatalytic activity over flower-like sphere Ag/Ag2CO3/BiVO4 plasmonic heterojunction photocatalyst for tetracycline degradation. Chem Eng J 331:242-254

Long M, Jiang J, Li Y et al. (2011) Effect of Gold Nanoparticles on the Photocatalytic and Photoelectrochemical Performance of Au Modified BiVO4. Nano-Micro Lett 3(3):171-177

Lopes OF, Carvalho KTG, Macedo GK et al. (2015) Synthesis of BiVO4 via oxidant peroxo-method: Insights into the photocatalytic performance and degradation mechanism of pollutants. New J Chem 39:6231-6237

Lopes OF, Carvalho KTG, Nogueira AE et al. (2016) Controlled synthesis of BiVO4 photocatalysts: Evidence of the role of heterojunctions in their catalytic performance driven by visible light. Appl Catal B 188:87-97

Lopez-Alvarez B, Torres-Plama RA, Penuela G (2011) Solar photocatalitycal treatment of carbofuran at lab and pilot scale: Effect of classical parameters, evaluation of the toxicity and analysis of organic by-products. J Hazard Mater 191:196-203

Lowry GV and Johnson KM (2004) Congener-Specific Dechlorination of Dissolved PCBs by Microscale and Nanoscale Zerovalent Iron in a Water/Methanol Solution. Environ Sci Technol 38:5208-5216

Lu YC, Chen CC, Lu CS (2014) Photocatalytic degradation of bis(2-chloroethoxy)methane by a visible light-driven BiVO4 photocatalyst. J Taiwan Inst Chem E 45:1015-1024

Lu Y, Shang H, Guan H et al. (2015) Enhanced visible-light photocatalytic activity of BiVO4 microstructures via annealing process. Superlattice Microst 88:591-599

Luo W, Yang Z, Li Z et al. (2011) Solar hydrogen generation from seawater with a modified BiVO4 photoanode. Energ Environ Sci 4:4046-4051

Luo Y, Tan G, Dong G et al. (2015a) Structural transformation of Sm3+ doped BiVO4 with high photocatalytic activity under simulated sun-light. Appl Surf Sci 324:505-511

Luo Y, Tan G, Dong G et al. (2015b) Effects of structure, morphology, and up-conversion on Nd-doped BiVO4 system with high photocatalytic activity. Ceram Int 41:3259-3268

Luo Y, Tan G, Dong G et al. (2016) A comprehensive investigation of tetragonal Gd-doped BiVO4 with enhanced photocatalytic performance under sun-light. Appl Surf Sci 364:156-165

Mohapatra L and Parida KM (2014) Dramatic activities of vanadate intercalated bismuth doped LDH for solar light photocatalysis. Phys Chem Chem Phys 16:16985-16996

Monfort O, Roch T, Gregor M et al. (2017a) Photooxidative properties of various BiVO4/TiO2 layered composite films and study of their photocatalytic mechanism in pollutant degradation. J Environ Chem Eng 5:5143-5149

Monfort O, Sfaelou S, Satrapinskyy L et al. (2017b) Comparative study between pristine and Nb-modified BiVO4 films employed for photoelectrocatalytic production of H2 by water

splitting and for photocatalytic degradation of organic pollutants under simulated solar light. Catal Today 280:51-57

Moniz SJA, Shevlin SA, Martin DJ et al. (2015) Visible-Light Driven Heterojunction Photocatalysts for Water Splitting - A Critical Review. Energ Environ Sci 8:731-759

Ni M, Leung MKH, Leung DYC et al. (2007) A review and recent developments in photocatalytic water-splitting using TiO2 for hydrogen production. Renew Sust Energ Rev 11:401-425

O'Carroll D, Sleep B, Krol M et al. (2013) Nanoscale zero valent iron and bimetallic particles for contaminated site remediation. Adv Water Resour 51:104-122

Obregon S and Colon G (2014) Heterostructured Er3+ doped BiVO4 with exceptional photocatalytic performance by cooperative electronic and luminescence sensitization mechanism. Appl Catal B 158-159:242-249

Odling G. and Robertson N (2016) BiVO4-TiO2 Composite Photocatalysts for Dye Degradation Formed Using the SILAR Method. ChemPhysChem 17(18):2872-2880

Park HS, Kweon KE, Ye H et al. (2011) Factors in the Metal Doping of BiVO4 for Improved Photoelectrocatalytic Activity as Studied by Scanning Electrochemical Microscopy and First-Principles Density-Functional Calculation. J Phys Chem C 115(36):17870-17879

Park Y, McDonald KJ, Choi KS (2013) Progress in bismuth vanadate photoanodes for use in solar water oxidation. Chem Soc Rev 42:2321-2337

Parmar KPS, Kang HJ, Bist A et al. (2012) Photocatalytic and Photoelectrochemical Water Oxidation over Metal-Doped Monoclinic BiVO4 Photoanodes. ChemSusChem 5:1926-1934

Pilosh Y, Turkevych I, Mawatari K et al. (2014) Nanostructured WO3/BiVO4 Photoanodes for Efficient Photoelectrochemical Water Splitting. Small 10(18):3692-3699

Pingmuang K, Chen J, Nattestad A et al. (2014) Photocatalytic Degradation of Methylene Blue by Innovative BiVO4/TiO2 Composite Films under Visible Light Irradiation. J Environ Sci 3(1):69-76

Polczynski P, Jurczakowski R, Grochala W (2013) Stabilization and strong oxidizing properties of Ag(II) in a fluorine-free solvent. Chem Commun 49:7480-7482

Pookmanee P, Kojinok S, Phanichphant S (2012) Bismuth Vanadate (BiVO4) Powder Prepared by the Sol-gel Method. J Met Mater Min 22(2):49-53

Quiroga JM, Riaza A, Manzano MA (2009) Chemical degradation of PCB in the contaminated soils slurry: Direct Fenton oxidation and desorption combined with the photo-Fenton process. J Environ Sci Health A 44(11):1120-1126

Ran R, McEvoy JG, Zhang Z (2015) Synthesis and Optimization of Visible Light Active BiVO4 Photocatalysts for the Degradation of RhB. Int J Photoenergy 2015:1-14

Regmi C, Kshetri YK, Kim TH et al. (2017) Visible-light-induced Fe-doped BiVO4 photocatalyst for contaminated water treatment. Mol Catal 432:220-231

Roth RS and Waring JL (1963) Synthesis and stability of bismutotantalite stibiotantalite and chemically similar ABO4 compounds. Am Mineral 48:1348-1356

Rybnikova V, Usman M, Hanna K (2016) Removal of PCBs in contaminated soils by means of chemical redeuction and advanced oxidation processes. Environ Sci Pollut Res 23(17):17035-17048

Saison T, Chemin N, Chaneac C et al. (2015) New Insights Into BiVO4 Properties as Visible Light Photocatalyst. J Phys Chem C 119(23):12967-12977

Sayama K, Nomura A, Zou Z et al. (2003) Photoelectrochemical decomposition of water on nanocrystalline BiVO4 film electrodes under visible light. Chem Commun 23:2908-2909

Seabold JA and Choi KS (2012) Efficient and Stable Photo-Oxidation of Water by a Bismuth Vanadate Photoanode Coupled with an Iron Oxyhydroxide Oxygen Evolution Catalyst. J Am Chem Soc 134(4):2186-2192

Selvarajan S, Suganthi A, Rajarajan M et al. (2017) Highly efficient BiVO4/WO3 nanocomposite towards superior photocatalytic performance. Powder Technol 307:203-212

Serpone N and Salinaro A (1999) Terminology, relative photonic efficiencies and quantum yields in heterogeneous photocatalysis. Part I: suggested protocol. Pure Appl Chem 71(2):303-320

Shan L, Mi J, Dong L et al. (2014) Enhanced Photocatalytic Properties of Silver Oxide Loaded Bismuth Vanadate. Chinese J Chem Eng 22:909-913

Shan L and Liu Y (2016) Er3+, Yb3+ doping induced core-shell structured BiVO4 and near-infrared photocatalytic properties. J Mol Catal A 416:1-9

Shen Y, Huang M, Huang Y et al. (2010) The synthesis of bismuth vanadate powders and their photocatalytic properties under visible light irradiation. J Alloy Compd 496:287-292

Song X, Li Y, Wei Z et al. (2017) Synthesis of BiVO4/P25 composites for the photocatalytic degradation of ethylene under visible light. Chem Eng J 314:443-452

Sun J, Li X, Zhao Q et al. (2015) Quantum-sized BiVO4 Modified TiO2 Microflower Composite Heterostructure: Efficient Production of Hydroxyl Radicals towards Visible Light-Driven Degradation of Gaseous Toluene. J Mater Chem A 3:21655-21663

Tachikawa T, Ochi T, Kobori Y (2016) Crystal-Face-Dependent Charge Dynamics on a BiVO4 Photocatalyst Revealed by Single-Particle Spectroelectrochemistry. ACS Catal 6(4):2250-2256

Tan G, Zhang L, Ren H et al. (2014) Microwave hydrothermal synthesis of N-doped BiVO4 nanoplates with exposed (040) facets and enhanced visible-light photocatalytic properties. Ceram Int 40:9541-9547

Tan HL, Wen X, Amal R et al. (2016) BiVO4 {010} and {110} Relative Exposure Extent: Governing Factor of Surface Charge Population and Photocatalytic Activity. J Phys Chem Lett 7(7):1400-1405

Tan HL, Suyanto A, Denko ATD et al. (2017) Enhancing the Photoactivity of Faceted BiVO4 via Annealing in Oxygen-Deficient Condition. Part Part Syst Char 34(4):1600290-1600299

Teoh WY, Scott JA, Amal R (2012) Progress in Heterogeneous Photocatalysis: From Classical Radical Chemistry to Engineering Nanomaterials and Solar Reactors. J Phys Chem Lett 3(5):629-639

Thalluri SM, Hussain M, Saracco G et al. (2014) Green-Synthesized BiVO4 Oriented along {040} Facets for VisibleLight-Driven Ethylene Degradation. Ind Eng Chem Res 53(7):2640-2646

Thurston JH, Trahan D, Ould-Ely T et al. (2004) Toward a General Strategy for the Synthesis of Heterobimetallic Coordination Complexes for Use as Precursors to Metal Oxide Materials: Synthesis, Characterization, and Thermal Decomposition of Bi2(Hsal)6.M(Acac)3 (M = Al, Co, V, Fe, Cr). Inorg Chem 43:3299-3305

Tokunaga S, Kato H, Kudo A (2001) Selective Preparation of Monoclinic and Tetragonal BiVO4 with Scheelite Structure and Their Photocatalytic Properties. Chem Mater 13(12):4624-4628

Tolod KR, Hernandez S, Russo N (2017) Recent Advances in the BiVO4 Photocatalyst for Sun-Driven Water Oxidation: Top-Performing Photoanodes and Scale-Up Challenges. Catalysts 7:13-36

Trzcinski K, Szkoda M, Sawczak M et al. (2016) Visible light activity of pulsed layer deposited BiVO4/MnO2 films decorated with gold nanoparticles: The evidence for hydroxyl radicals formation. Appl Surf Sci 385:199-208

Wang M, Zheng H, Liu J et al. (2015) Enhanced visible-light-driven photocatalytic activity of B-doped BiVO4 synthesized using a corn stem template. Mat Sci Semicon Proc 30:307-313

Wang X, Shen Y, Zuo G et al. (2016) Influence of heat treatment on photocatalytic performance of BiVO4 synthesised by sol-gel method. Mater Technol 31(3):176-180

Wang M, Guo P, Chai T et al. (2017a) Effects of Cu dopants on the structures and photocatalytic performance of cocoon-like Cu-BiVO4 prepared via ethylene glycol solvothermal method. J Alloy Compd 691:8-14

Wang M, Yang GJ, You MY et al. (2017b) Effects of Ni doping contents on photocatalytic activity of B-BiVO4 synthesized through sol-gel and impregnation two-step method. Trans Nonferrous Met Soc China 27:2022-2030

Wetchakun N, Chainet S, Phanichphant S et al. (2015) Efficient photocatalytic degradation of methylene blue over BiVO4/TiO2 nanocomposites. Ceram Int 41(4):5999-6004

Wood PM (1988) The potential diagram for oxygen at pH 7. Biochem J 253:287-289

Xi G and Ye J (2010) Synthesis of bismuth vanadate nanoplates with exposed {001} facets and enhanced visible-light photocatalytic properties. Chem Commun 46:1893-1895

Xue S, He H, Wu Z et al. (2017) An interesting Eu,F-codoped BiVO4 microsphere with enhanced photocatalytic performance. J Alloy Compd 694:989-997

Xu YH, Liu CJ, Chen MJ et al. (2011) A review in visible-light-driven BiVO4 photocatalysts. Int J Nanopart 4(2/3):268-283

Xu X, Zou Q, Yuan Y et al. (2014) Preparation of BiVO4-graphene Nanocomposites and Their Photocatalytic Activity. J Nanomater 2014:1-6

Xu X and Song W (2017) Synthesis and photocatalytic activity of heterojunction ZnFe2O4-BiVO4. Mater Technol 32(8):472-479

Ye H, Lee J, Jang JS et al. (2010) Rapid Screening of BiVO4-Based Photocatalysts by Scanning Electrochemical Microscopy (SECM) and Studies of Their Photoelectrochemical Properties. J Phys Chem C 114(31):13322-13328

Yuan Q, Chen L, Xiong M et al. (2014) Cu2O/BiVO4 heterostructures: synthesis and application in simultaneous photocatalytic oxidation of organic dyes and reduction of Cr(VI) under visible light. Chem Eng J 255:394-402

Yuan X, Zhang G, Yang X et al. (2016) Preparation of BiOBr/BiVO4 composite and its application for photocatalytic degradation under visible light. Mater Res Innov 20(3):230-234

Zhai Y, Yin Y, Liu X et al. (2017) Novel Magnetically Separable BiVO4/Fe3O4 Photocatalyst: Synthesis and Photocatalytic Performance under Visible-light Irradiation. Mater Res Bull 89:297-306

Zhang S, Zheng Z, Wang J et al. (2006) Heterogeneous photocatalytic decomposition of benzene on lanthanum-doped TiO2 film at ambient temperature. Chemosphere 65(11):2282-2288

Zhang X, Zhang Y, Quan X et al. (2009) Preparation of Ag doped BiVO4 film and its enhanced photoelectrocatalytic (PEC) ability of phenol degradation under visible light. J Hazard Mater 167:911-914

Zhang M, Shao C, Li X et al. (2012) Carbon-modified BiVO4 microtubes embedded by Ag nanoparticles with high photocatalytic activity under visible light. Nanoscale 4(23):7501-7508

Zhang B, Li J, Zhang B et al. (2015) Selective oxidation of sulfides on Pt/BiVO4 photocatalyst under visible light irradiation using water as the oxygen source and dioxygen as the electron acceptor. J Catal 332:95-100

Zhang K, Liu Y, Deng J et al. (2018) Co-Pd/BiVO4: High-performance photocatalysts for the degradation of phenol under visible light irradiation. Appl Catal B 224:350-359

Zhou L, Wang W, Liu S et al. (2006) A sonochemical route to visible-light-driven high-activity BiVO4 photocatalyst. J Mol Catal A 252:120-124

Zhou B, Zhao X, Liu H et al. (2010) Visible-light sensitive cobalt-doped BiVO4 (Co-BiVO4) photocatalytic composites for the degradation of methylene blue dye in dilute aqueous solutions. Appl Catal B 99(1-2):214-221

Zhu Z, Han Q, Yu D et al. (2017a) A novel p-n heterojunction of BiVO4/TiO2/GO composite for enhanced visible-light-driven photocatalytic activity. Mater Lett 209:379-383

Zhu Y, Shah MW, Wang C (2017b) Insight into the role of Ti3+ in the photocatalytic performance of shuriken-shaped BiVO4/TiO2-x heterojunction. Appl Catal B 203:526-532